A Study of the Effect of Group Delay Distortion on an SMSK Satellite Communications Channel

Robert J. Kerczewski
Lewis Research Center
Cleveland, Ohio

April 1987

NASA

A STUDY OF THE EFFECT OF GROUP DELAY DISTORTION

ON AN SMSK SATELLITE COMMUNICATIONS CHANNEL

Robert J. Kerczewski
National Aeronautics and Space Administration
Lewis Research Center
Cleveland, Ohio 44135

SUMMARY

The effects of group delay distortion on an SMSK satellite communications channel have been investigated. Software and hardware simulations have been used to determine the effects of channel group delay variations with frequency on the bit error rate for a 220 Mbps SMSK channel. These simulations indicate that group delay distortions can significantly degrade the bit error rate performance. The severity of the degradation is dependent on the amount, type, and spectral location of the group delay distortion.

1. INTRODUCTION

Over the past seven years, work in advanced communications technology at NASA Lewis Research Center has focused on Ka-band satellite communications systems. The intent of this research is to improve the efficiency of satellite communications systems through development of multi-beam antenna systems, satellite switching and processing technology, TDMA networking concepts, cost-efficient ground terminals, improved modulation methods, and other techniques. The work done at NASA Lewis, in addition to sponsoring hardware development through contracts with industry, includes system development, hardware testing and characterization, and laboratory experimentation with systems designed and developed in-house.

In the area of digital modulation technology, much work has been done by NASA Lewis in sponsoring the development of modulators and demodulators (modems) using serial minimum shift keyed (SMSK) modulation. This type of modulation will also be used for NASA's Advanced Communications Technology Satellite flight project. Characterization of the performance of a satellite communications channel using SMSK modulation has thus been a significant part of the in-house research program at Lewis.

The performance of such a satellite communications channel in the presence of group delay distortion is examined in this report. Using computer simulations and measured results, the effects of various types of group delay distortions are analyzed and presented.

2. SMSK MODULATION CONSIDERATIONS

Minimum-shift-keyed (MSK) modulation is a quadrature-type digital modulation scheme where the two data channels (I and Q channels, see fig. 1) are staggered by one-half the bit rate, bi-phase modulated, and weighted by a half-sinusoid. The result is a modulation which performs similarly to other quadrature modulations (such as quadrature-phase-shift keying (QPSK) and offset

QPSK) in that the ratio of energy per bit to noise power (E_b/N_0) required to maintain a given bit error rate (BER) is identical (ref. 13). The advantage of MSK compared to other quadrature modulations is its higher bandwidth efficiency. SMSK modulation requires a smaller amount of channel bandwidth to transmit data at a given rate than other modulation techniques. For example, the 99 percent bandwidth (the amount of bandwidth which contains 99 percent of the signal energy) for MSK is 1.18 times the bit rate of the digital data being modulated, while for QPSK modulation, the 99 percent bandwidth is 10.28 times the bit rate (refs. 3 and 2). This is due to the fact that MSK modulation contains a significantly higher percentage of its power near the center of its power spectrum, as demonstrated by the fractional out-of-band power plots for PSK, QPSK, and MSK modulation shown in figure 2 (ref. 3).

For the reasons stated above, namely good E_b/N_0 performance and bandwidth efficiency, MSK modulation is an important development in the attempt to improve the efficiency of digital satellite communication systems. NASA Lewis has sponsored the development of high data rate modulators and demodulators using serial MSK modulation. At high data rates, problems with time synchronization, and maintaining amplitude and phase quadrature make this alternate method of MSK modulation more attractive. Figure 3 shows a block diagram of a serially-implemented MSK modulator where the data is bi-phase modulated serially and then covered to an MSK format by a bandpass conversion filter with a sin (x)/x-shaped transfer function (ref. 13). This filter is offset from the center frequency by one-fourth of the data rate. This results in the carrier appearing at one-fourth the data rate below the center frequency of the modulation spectrum. A comparison of figures 1 and 3 shows the relative simplicity of the serial minimum shift keyed (SMSK) implementation.

The SMSK modulators and demodulators built under the NASA-sponsored program operate at a data rate of 221.184 Mbps. As shown in figure 4, the main lobe of the SMSK power spectrum at this data rate is 330 MHz wide. Good BER performance can be obtained in a bandlimited system by transmitting only this main lobe, as will be shown later. The 330 MHz bandwidth is used for all simulations and measurements described in this report.

3. SITE SATELLITE COMMUNICATION SYSTEM SIMULATOR

The investigation of the effects of group delay distortion include measurements made in the NASA Lewis Systems Integration, Test and Evaluation (SITE) Laboratory. In the SITE Lab, a hardware-based satellite communication system link simulator has been constructed using Ka-Band communication system hardware developed by a variety of contractors under NASA-sponsored technology development programs. Figure 5 describes the system, which includes satellite receivers, power amplifiers, a microwave matrix switch, the SMSK modems described above, and ground terminal upand down-converters. The rest of the hardware shown in the diagram (noise insertion, data generators and checkers, and control computer) are the result of in-house developments.

The intent of the SITE satellite system simulator is to provide a test bed for a variety of digital satellite communication system measurements and experiments. Since all of the hardware used has been designed to meet satellite system requirements, the simulator provides a real environment for observing many of the effects of an operational system. Under computer control, the system is capable of performing a variety of automated BER and

unmodulated continuous wave (CW) measurements (ref. 19). In particular, the group delay and BER versus E_b/N_o measurements described below are performed using this system.

The hardware comprising the SITE satellite communication system simulator allow a large number of system variations to be obtained. Two satellite high power amplifiers are available, a traveling wave tube amplifier (TWTA) and a solid state (GaAsFET) amplifier. The TWTA can be operated in three power modes. In addition, the matrix switch contains 66 populated crosspoints, each with different transmission characteristics. All of the components have been designed to operate over a bandwidth of 2.5 GHz, allowing a number of 330 MHz SMSK channels to be obtained.

In all of the SITE testing to date, the following combinations of conditions have been set.

(1) The TWTA is operated in each of the three power modes.
(2) The TWTA and GaAsFET are operated at saturation, the 1 dB power compression point, and in the linear region.
(3) Three frequency bands (or channels), as defined in figure 6, are used for testing.
(4) One primary matrix switch crosspoint and one 4x4 block of crosspoints (to be used in dynamic switching tests) are used for testing, for a total of 17 crosspoints.

This leads to a total of 612 possible test combinations. Only a portion of this total is used for the tests described in this report.

4. MEASUREMENT OF SYSTEM GROUP DELAY

In order to determine the magnitude and type of group delay variations which might be expected in a 30/20 GHz satellite communication system, group delay measurement techniques were developed and applied to the SITE 30/20 GHz communication system simulator. The measurement technique used, and the results of measurements made on the SITE system are described in the following paragraphs. It should be noted that the SITE simulator does not include the effects of signal propagation over a 22 400 mile satellite upand downlink from geosynchronous orbit. The group delay measurements made reflect only the distortions caused by the satellite transponder and ground terminal hardware.

4.1 MEASUREMENT TECHNIQUE

The group delay of a system is defined as .the negative of the derivative of the phase of the system with respect to frequency (ref. 3), as shown in figure 7.

$$T_d = \frac{d\varphi}{dw}$$

where

T_d group delay
φ the system phase at frequency w

Thus, the group delay is a measure of the linearity of the system's phase response. A linear phase response (corresponding to a constant group delay) causes no transmission distortion in the system. Group delay can therefore be an important parameter in determining the transmission quality of a system.

The simplest and most direct method for measuring the end-to-end system group delay is to measure the phase shift from system input to system output, using a microwave network analyzer, for a number of frequencies across the passband of interest. The group delay can be derived from the phase measurements by calculating the slope between phase points (fig. 7). This direct method is well suited to devices and systems which do not perform frequency translations. Unfortunately, in the SITE single channel transponder, a number of frequency translations are performed (as shown in fig. 5) using oscillators that are not phase-locked to one another. The instability and frequency drift of the various oscillators results in a system output signal that is varying in frequency with respect to the input signal. Such variations prevent an accurate phase shift measurement.

An alternate, indirect method of group delay measurement, which is not affected by frequency translations, was found to be applicable to the SITE system. In this method, a CW test signal is amplitude modulated and passed through the system under test. The phase shift of the detected amplitude envelope is measured from system input to output and is mathematically related to the group delay (Appendix A1) by

$$T_d = \frac{\varphi_e}{(360° \times f_m)}$$

where

T_d group delay in sec
φ_e modulation phase shift in deg
f_m modulation frequency in Hz

In implementing this equation, it is noted that the modulation frequency represents a "window" of width $2f_m$ over which the group delay measurement is essentially being averaged (fig. 8 and appendix A1). Thus, accurate measurements require that f_m be kept as small as possible. Reducing f_m, however, has the effect of reducing the resolution of the device measuring the envelope phase shift. For example, choosing $f_m = 1$ MHz gives an instrument resolution of 2.778 nsec of group delay per degree of phase shift. $f_m = 10$ MHz gives 0.2778 nsec/deg. Since the group delay measurements will be made over a channel bandwidth of 330 MHz, the measurement window can be several MHz wide and still give a measurement frequency resolution of about 0.01 of the measurement bandwidth. The resolution of the phase meter used to measure the envelope phase shift (Hewlett-Packard 8405A Vector Voltmeter) is 0.1° (ref. 5). Thus, a good compromise between measurement window width and measurement resolution is to choose $f_m = 2.778$ MHz. This choice has the additional benefit of giving a direct phase meter reading of 1° of envelope phase shift equal to 1 nsec of group delay.

The group delay measurement method described above is usually performed in a swept frequency fashion, with the group delay (from the phase meter output) plotted on an X-Y recorder vs. frequency. Such measurements are difficult

4

to assess accurately, since the absolute value of the measurement is dependent upon previously drawn calibration curves which often have large variations from linearity. The measurement is greatly improved by adding a digital voltmeter and control computer to the measurement setup.

Figure 9 shows the final configuration for the group delay measurement. The control computer steps the CW signal source through a number of frequencies across the passband of interest. The amplitude modulation is provided by a PIN diode switch and the envelope is detected at the system output with a crystal detector. The phase shift between the test signal (from the detector) and the reference signal (from the 2.778 MHz modulation source) is measured by the vector voltmeter. The vector voltmeter's phase meter provides a voltage output proportional to the measured phase shift. This voltage is read by the digital voltmeter and is made available to the control computer. The control computer converts this voltage reading to a group delay measurement at the frequency of the CW signal source. A calibration measurement is made by removing the system under test from the measurement setup. The computer stores this calibration data and subtracts it from the measured data as the measurement is being made on the system. This gives a corrected group delay measurement. In addition, multiple measurements can be made at a given frequency and averaged to reduce the effects of system noise on the measurement accuracy.

The group delay measurement system gives results that are accurate to within ±2.5 nsec. Measurement accuracy considerations are discussed in appendix A1.

4.2 RESULTS

A typical plotted output of the group delay measurement computer program is shown in figure 10. Table 1 summarizes the results of group delay measurements on the SITE satellite communication system simulator for 72 selected cases. The 72 cases represent a sample of the 612 test combinations described in section 3, with roughly equal samples of all amplifiers, power modes, frequency bands, and crosspoints. The measurement result listed is the maximum peak-to-peak deviation in the 330 MHz band, measured as indicated in figure 10.

As Table I shows, the average group delay variation for the 72 samples is 4.72 nanaoseconds, with a standard deviation of 3.70 nsec. The shape of the measured group delay curves varies greatly from sample to sample. In general, though, they can be characterized as combinations of one or more of the following shapes: linear slope (positive or negative), exponential slope (either a concave or convex parabolic shape), positive or negative "spike," and nonperiodic ripple. Nearly all of the samples have some small amount (usually less than 1 nsec) of nonperiodic ripple combined with one or more of the other shapes.

The general shapes mentioned above form the basis for the computer simulations described in section 5.

5.0 COMPUTER SIMULATION OF GROUP DELAY EFFECTS

A simulation of the effects of certain types of group delay distortions was performed using a computer program available and in use at NASA Lewis

5

called the Channel Model Simulation Program (CMSP). The CMSP models a satellite communications channel and allows the effects of numerous transmission impairments and configurations to be observed.

The purpose of the computer simulation was to observe the effects of group delay distortion on the BER of an SMSK digital satellite communication channel. The output of the simulation was a number of BER versus E_b/N_0 curves representing the performance of an SMSK channel under various group delay distortions. These curves indicate the general trends of the distortion effects and are not intended to be quantitative measurements of the degradation caused by group delay distortion. Numerous other transmission impairments which occur in a real system, such as nonlinearities, phase noise, amplitude distortion, and AM/PM conversion, are not taken into account. All of these distortions, as well as the interaction between them, have an effect on the system performance (refs. 17 and 18). The difficulty in accurately measuring and modeling these other effects makes it unrealistic to attempt to do so within the scope of the work reported here. Thus, group delay distortion is the only distortion modeled in the simulations. The distortions used are those observed to exist in the SITE communications system simulator, described in section 4.2.

5.1 CMSP DESCRIPTION

The CMSP is designed to simulate the performance of a digital satellite communications link. The primary program output is a calculation of the probability of bit error as a function of E_b/N_0 for a given link configuration.

The program performs the simulation based on a sampled time domain representation of the transmitted signals and the transformations the signals undergo as they pass through the modeled system. The system model must include a transmitter (modulator) and receiver (demodulator), and may also include filters, nonlinear elements, noise insertion, interference, and satellite on-board processing. The simulation configuration capabilities are shown in figure 11 (from ref. 16).

The configuration used for the group delay simulations include a transmitter (random data source with no coding and SMSK modulator), filter 7 (see fig. C1) through which the group delay distortion was introduced, and the receiver (SMSK demodulator and data detector). A completely linear channel was modeled, and none of the other system options were exercised. The program options allow the user to simulate any type of filter, whether or not it is physically realizable, by specifying a frequency sampled amplitude and phase response. In this way, a filter with a flat amplitude response and distorted group delay response was specified as part of the simulation in order to observe only the effects of the group delay distortion.

5.2 GROUP DELAY PROFILES

Eleven group delay distortions were simulated. The profiles of these distortions as plotted over the 330 MHz bandwidth are shown in figure 12. Linear slope (positive and negative), exponential slopes (convex and concave-shaped parabolic), ripple, spikes at the center of the band (positive and negative), and spikes varied in spectral location across the band (positive

6

and negative) were simulated, paralleling the types of group delay distortions measured in the SITE satellite communications system simulator. The first profile is a flat (distortionless) group delay, used as an experiment control.

Each of the group delay distortions was modeled in one nanosecond increments, with the distortion increasing until severe degradation of the BER was observed. Severe degradation is considered to be an increase of at least 8 dB in the E_b/N_0 required to maintain a BER of 5×10^{-7}.

In order to model the group delay distortions, they first must be converted to phase samples. This is done by integrating the group delay to obtain the phase shift, as shown in figure 13. The measured group delay samples (representing the slope of the phase response) are first converted to phase shifts by multiplying the group delay by the measurement interval. The average phase shift between intervals is added to the previous phase point to yield a set of phase shift points which correspond to the desired group delay distortion and can be used for the filter phase response in the CMSP simulation. The phase responses are shown in figure 12 with the corresponding group delay profiles.

5.3 CMSP EXECUTION

The construction of a CMSP input data set for the group delay distortion simulation is described in appendix A2. Once an input data set has been constructed and identified, the simulation program can be executed. The result is an output of a table of BER versus E_b/N_0, as shown in figure 15. The theoretical, or ideal, SMSK curve is also given by the CMSP.

One important parameter that affects the calculated BER results is the receiver phase offset. The receiver and transmitter are initially phase-locked. The phase offset allows a compensation for the phase distortions introduced into the simulated channel. Since the optimum phase offset varies (from 0 to 2π rad) for each distortion simulated, an average of about 10 iterations are required to find the optimum phase offset for each simulation.

5.4 RESULTS

The primary output of the CMSP is a table of BER versus E_b/N_0. A computer program called "BERPLOT" was developed in store, analyze, and plot BER versus E_b/N_0 data resulting from the CMSP simulations and from BER measurements described later in this report. The program yields a plot of the BER versus E_b/N_0 data, as shown in figure 16 for the positive group delay slope simulations. Figure 16 demonstrates the effect that a varying group delay slope has on the system's characteristic BER curve. For example, it can be seen that an increase of the group delay slope results in the BER curve moving to the right on the plot. This corresponds to a poorer system response since a larger E_b/N_0 is required to maintain a given BER. A quantitative measure of the magnitude of the system degradation caused by the group delay distortion is the E_b/N_0 required to maintain a given BER as compared to the theoretical SMSK curve. This degradation can be plotted against the magnitude of the group delay distortion, using the BERPLOT program, to give a clear picture of the effects of the distortion on the system BER. The standard BER chosen for E_b/N_0 comparison in this report is 5×10^{-7}.

The E_b/N_0 are calculated using a linear interpolation between points. The E_b/N_0 for the theoretical curve is calculated and subtracted from the E_b/N_0 for the simulation curve, resulting in an E_b/N_0 degradation measurement. Examples of such curves are figures 17 to 22.

The results of the group delay distortion simulations show a number of effects. Both the magnitude and spectral location of a given distortion were found to be important in terms of the degradation observed. The E_b/N_0 degradations are plotted in figures 17 through 22 for the flat, linear slope, expotential (parabolic), spike, and ripple group delay distortions. These results are now explained.

The experiment control applied to these simulations was a flat group delay. As explained in section 4.1, a flat group delay presents no distortion. Therefore, placing a flat group delay in filter 7 for the CMSP simulation should ideally result in no E_b/N_0 degradation. Such a simulation was performed using flat group delays ranging from 0 to 10 nsec in 1 nsec steps. The resulting E_b/N_0 degradation at a BER of 5×10^{-7} for the 11 simulations is plotted in figure 17. As expected, the flat group delay caused very little E_b/N_0 variation from the 0 nsec group delay curve (the variation was from -0.14 to +0.20 dB). At 10 nsec, the simulation was apparently no longer able to compensate for the large additional phase shift (amounting to 37 rad at the last frequency sample) being introduced into the channel. The control experiment results indicate that for phase shifts less than 37 rad, the CMSP is providing a reasonably good simulation. The only distortion simulated in which a larger phase shift was introduced was the convex parabolic group delay (above 17 nsec).

In figure 18, the results of positive and negative linear slope group delay distortion simulations are plotted. The positive slope introduces a much larger degradation than the negative slope. For example, for a 5 nsec slope, the negative slope degrades the performance by 2 dB while the positive slope degradation is 5 dB. This difference can be accounted for by the shape of the phase shift being added in the simulation. Figure 12 shows that the negative slope adds a phase shift which tends to reduce the slope of the overall system phase response, while the positive slope adds a phase shift which increases the slope of the system phase response.

The parabolic and inverse parabolic (or concave and convex) group delay distortions are shown in figure 12. The inverse parabolic distortion was expected to cause a greater system E_b/N_0 degradation since the largest group delays (and corresponding phase shifts) occur at the center of the band, where most of the signal power is concentrated. The parabolic group delay distortion has the highest group delays (and phase shifts) occuring at the band edges, where very little signal power exists. Figure 19 confirms this expected result, showing a much greater degradation caused by the inverse parabolic group delay than by the parabolic group delay. The channel becomes unusable at a inverse parabolic group delay of 14 nsec, while for the parabolic group delay, the channel can tolerate 24 nsec. It is also interesting to note that a parabolic group delay is often seen in channel bandpass filters. This simulation demonstrates the high tolerance of the SMSK modulation to such filter distortion.

In figure 20, the results for a positive and negative group delay spike, placed at the center of the frequency band, are shown. The positive spike

8

causes over 7 dB greater degradation than the negative spike at a spike amplitude of 4 nsec, while for a negative spike, 12 nsec was required. Figure 12 shows the phase response for the positive and negative spikes. The phase distortion is much more abrupt for the positive spike than for the negative spike.

After examining the results of the center frequency spike simulations, a 3 nsec positive spike and 7 nsec negative spike (both yielding a 4 dB E_b/N_0 degradation from theoretical) were moved across the entire 330 MHz band in ten steps. The results of these simulations are plotted in figure 21. The degradation due to the positive spike remains constant over most of the band, with one maximum occurring at about 55 MHz above the center frequency. The negative spike has two maxima, one occurring at 55 MHz below the center frequency and the other at about 55 MHz above the center frequency. For MSK-type modulation, the instantaneous frequency transmitted when a series of all 1's or all 0's is modulated is one fourth the bit rate below the center frequency, while the instantaneous frequency when a 1-0-1-0...series is modulated is one fourth the bit rate above the center frequency (ref. 13). For modems operating at 220 Mbps, one fourth the data rate equals 55 MHz. Thus the effect of the group delay spikes occurring near these frequencies is to hinder the correct demodulation when consecutive bits are the same (for the case of spikes around 55 MHz below the center frequency) or when consecutive bits are different (for the case of spikes around 55 MHz above the center frequency).

The final group delay distortions simulated were a periodic ripple and a nonperiodic ripple, as shown in figure 12. The results of these simulations are plotted in figure 22. The periodic ripple caused a rapid degradation in the E_b/N_0, with no more than 2 nsec of distortion tolerable by the channel. The non-periodic distortion was less severe, with up to 5 nsec being tolerated before the channel was completely degraded. In examining figure 12 again, it is seen that the parabolic ripple introduces a distortion similar to the previously discussed negative spikes at 55 MHz above and below the center frequency. As shown, distortions at these frequencies cause severe degradation. The nonperiodic ripple also introduces distortions similar to the positive and negative spikes, but they are not located exactly at the critical ±55 MHz frequencies, leading to a less severe degradation.

The following conclusions can be drawn from the group delay distortion simulations. Distortions which occur near the center of the band, where most of the modulated signal power is located, cause more serious degradation of the system than distortions which occur at the band edges. The amount of degradation is related to the severity of the phase shift resulting from the group delay distortion. Finally, distortions which occur near plus or minus one-fourth the bit rate from the center frequency caused serious degradation to the SMSK channel.

6.0 SYSTEM BIT-ERROR RATE MEASUREMENTS

Measurements of the BER as a function of E_b/N_0 have been performed on the SITE satellite communication system simulator, using measurement techniques described below. A sample of the results of these measurements is given for 54 of the system configurations for which group delay measurement results were presented in section 4.2 (BER measurements with the GaAsFET power amplifier were not available at the time this report was prepared). An examination

9

is made of the apparent effects of the measured group delay on the measured system BER performance.

6.1 MEASUREMENT TECHNIQUE

The measurement of BER versus E_b/N_0 is accomplished under computer control, as shown in figure 5. The computer controls the ground terminal's data generator and checker and noise insertion hardware, and monitors the resulting BER and E_b/N_0.

Pseudo-random data at a rate of 220 Mbps is generated and sent to the modulator, from which an SMSK-modulated signal centered at 3.373 GHz is obtained. This signal is routed to ground terminal upconverters and shifted to the desired frequency band. The signal is then transmitted through the satellite transponder, where the desired matrix switch crosspoint and HPA power mode and drive level are selected. The signal then enters the ground terminal downconverter where it is translated back to a center frequency of 3.373 GHz. Before entering the demodulator, Gaussian (white) noise is added to the signal, the resulting signal to noise ratio is measured and the corresponding energy-per-bit to noise ratio (E_b/N_0) is calculated. The signal with the noise added is then demodulated and the resulting 220 Mbps bit stream is compared to a regenerated version of the original data stream. The errors are counted and the bit error rate is calculated. The amount of noise added is varied in 1 dB increments, resulting in a set of BER versus E_b/N_0 data which characterize the performance of the particular channel.

6.2 RESULTS

The results of the sample of 54 BER measurements are given in Table II. The BER parameter shown is the E_b/N_0 degradation from the theoretical SMSK curve at a BER of 5×10^{-7}. The average E_b/N_0 degradation is 2.5 dB, ranging from 0.79 to 7.15 dB. The degradation was less than 1.5 dB in 22 of the cases, indicating that very good BER performance can be achieved by transmitting only the main lobe of the SMSK spectrum.

The effect of the measured group delay distortion on the measured BER performance is difficult to identify precisely. In figure 23, the E_b/N_0 degradation is plotted against the maximum peak-to-peak group delay variation for the 54 cases. A straight line fit to these points has been calculated to be E_b/N_0 degradation from ideal [dB] = 1.164 + 0.341 (group delay variation [nsec]), at BER = 5×10^{-7} and this line has been plotted in figure 23. Thirty of the 54 points fall within ±1 dB of this line, while 26 of the points are within ±2 nsec. The considerable scatter of the points from the calculated line indicates that a number of factors contribute to BER performance degradation besides the group delay. These factors likely include the amplitude response, AM to PM conversion, nonlinearities, and noise and spurious signals of the system (ref. 18). In addition, the group delay parameter used for this comparison, the maximum peak-to-peak variation over the 330 MHz band, does not contain any details of the particular group delay distortion. The simulations described in section 5 have indicated the importance of not only the magnitude but also the type and location of the group delay distortion in determining the effect of the distortion on the BER performance. Still, the data in table I and II, as portrayed in figure 23, support the conclusion that the

group delay distortion in an SMSK communications channel significantly effects the BER performance, and that the performance degradation is related to the magnitude of the distortion.

7.0 COMPARISON OF PREDICTED AND MEASURED RESULTS

The measured BER performance of the SITE satellite communications system simulator was compared with the CMSP-predicted performance for ten system configurations. The configurations chosen for this comparison included only those with the HPA in the linear operating region in order to remove the nonlinear distortions from the system. The only distortion included in the CMSP model was the group delay distortion. The ten system configurations were chosen to give a variety of group delay responses.

The group delay distortions as measured for the system and input to the CMSP are shown in figure 24. Also plotted in figure 24 are the corresponding predicted and measured BER curves for each configuration.

For six of the ten cases tested, the difference between the predicted and measured BER curves (at BER = 5×10^{-7}) was less than 0.65 dB, which is a reasonably good prediction. For the other four cases, the difference ranged from 1.5 to 3.7 dB. Three of the four large differences occurred for frequency band C, where the group delay variation is greater than for the other two bands. In addition, band C has been observed to contain large amplitude variations which, while not included in the CMSP models, undoubtedly contribute to the measured BER degradation and thus account for some of the difference between the measured and predicted curves. For band A (with the TWTA in the high mode) a large amount of noise present in the channel may account for the difference between measured and predicted results.

Overall, for channels which do not contain any large transmission distortions, the CMSP model gives reasonably good predicted results based upon the group delay distortion present.

8.0 CONCLUSIONS

The group delay response of a digital satellite communication channel has a significant effect on the transmission quality of the channel as measured by the bit error rate. By employing an amplitude modulation technique, group delay measurements were made on the SITE satellite communication system simulator for a number of system configurations and operating points. These measurements have shown that a satellite channel, excluding the propagation effects, may have group delay variations ranging from 1 to 20 nsec (peak-to-peak), with an average measured variation of 4.72 nsec. The variations measured included linear and parabolic components, spikes, and ripples, and various combinations of these shapes. Since a constant (flat) group delay response induces no transmission degradation, these variations represent potential distortion to the channel.

The effect of the group delay distortion on an digital satellite channel employing serial minimum-shift keyed modulation has been studied. Such a channel, operating at a data rate of 220 Mbps (with a channel bandwidth of

330 MHz), has been simulated in software (using the Channel Model Simulation Program) and in hardware (using the SITE satellite communication system simulator).

The software simulations have indicated that the amount of degradation to the system BER is dependent upon the type of group delay variation, the severity of the variation, and, in particular, the location (in frequency) of the variation with respect to the SMSK spectrum. Near the band edges, a variation of up to 12 nsec can be tolerated with less than 1 dB of additional E_b/N_o required to maintain a BER of $5x10^{-7}$. This result is significant, since it indicates that an SMSK channel may not require equalization for channel bandpass filters which contain a parabolic group delay response. Near the center of the band, however, a group delay variation of 4 nsec may cause over 8 dB of degradation. Areas particularly sensitive to group delay variation are the frequencies located at plus or minus one-fourth times the bit rate from the center frequency. These frequencies correspond to the instantaneous modulator outputs occurring when either constant or alternating bits (all 1's or 0's, or a 1-0-1-0... sequence) are input to the modulator. The measured BER results discussed below indicate that as group delay variations in a channel increase, other transmission impairments also increase and further degrade the channel's performance. Thus, in a real system, the tolerable group delay variations, when coupled with other expected system impairments, will be somewhat lower than these simulations indicate

The hardware simulations consisted of BER versus E_b/N_o measurements made on the SITE satellite communication system simulator. The degradation of the E_b/N_o at a BER of $5x10^{-7}$ was compared to the measured group delay variation for 54 systems configurations. The group delay variation parameter (peak-to-peak variation across the band) does not yield the details of the particular variation, such as the type or frequency location of the variation. In addition, the SITE simulator contains a number of other transmission impairments, such as amplitude variation, nonlinearities, and AM/PM conversion. However the comparison indicated a clear relationship between the amount of measured group delay variation and the measured E_b/N_o degradation. A straight line fit to the data showed that the additional E_b/N_o degradation (in dB) resulting from group delay variation was equal to 0.341 times the variation in nsec. The deviation from this straight line increased with the group delay variation, indicating that the effect of other transmission impairments increases as the group delay variation increases.

The BER performance of 10 SITE simulator configurations was predicted by the CMSP, based only on the measured group delay response. Comparing these predictions with the measured BER versus E_b/N_o curves shows that a good prediction can be made by the CMSP for channels with relatively low group delay distortions (3 nsec or less). As indicated by the 54 BER measurements discussed above, other transmission distortions become significant in channels with large group delay variations. This effect should be taken into account when considering the results of the CMSP simulations.

12

APPENDICES

A.1 GROUP DELAY MEASUREMENT TECHNIQUE AND ACCURACY CONSIDERATION

The derivation of the mathematical formula for group delay measurement, using the technique described in this report, is given in reference 8. It is repeated here with some details added, and with additional comments on the effects of carrier phase noise.

The amplitude modulated test signal at the system input is

$$e_1(t) = E_1(1 + M \sin W_m t) \sin W_c t) = E_1 \sin W_c t$$

$$+ \left(\frac{M}{2}\right) E_1 \cos \left(W_c - W_m\right) t - \left(\frac{M}{2}\right) E_1 \cos \left(W_c + W_m\right) t \qquad (A1)$$

where

M   modulation index
W_m modulation frequency
W_c carrier frequency

Assuming a constant group delay (T_d) from ($W_c - W_m$) to ($W_c + W_m$) (see fig. 8), the signal at the system output is

$$e_2(t) = E_2 \sin (W_c t + W_c T_d) + \left(\frac{M}{2}\right) E_2 \cos \left[(W_c - W_m)t + (W_c - W_m)T_d\right]$$

$$- \left(\frac{M}{2}\right) E_2 \cos \left[(W_c + W_m)t + (W_c + W_m)T_d\right] \qquad (A2)$$

The equation can be rearranged as follows.

$$e_2(t) = E_2 \sin W_c(t + T_d) + \left(\frac{M}{2}\right) E_2 \cos \left[W_c(t + T_d) - W_m(t + T_d)\right]$$

$$- \left(\frac{M}{2}\right) E_2 \cos \left[W_c(t + T_d) + W_m(t + T_d)\right] \qquad (A3)$$

$$e_2(t) = E_2 \left[1 + M \sin W_m(t + T_d)\right] \sin W_c(t + T_d) \qquad (A4)$$

$$e_2(t) = E_2 \left[1 + M \sin (W_m t + W_m T_d)\right] \sin (W_c t + W_c T_d) \qquad (A5)$$

The second term in parentheses in Equation (A5), ($W_c t + W_c T_d$), represents the carrier phase, with $W_c T_d$ representing the part of the carrier output phase due to group delay. The first term in parentheses, ($W_m t + W_m t_d$), represents the phase of the modulation envelope, with $W_m T_d$ representing the part due to the group delay (T_d). Comparing equation (A1) with equation (A5), the phase shift of the modulation envelope from system input to system output is

$$(W_m t + W_m T_d) - W_m t = W_m T_d \qquad \text{(A6)}$$

It is this quantity, $W_m T_d$, that can be easily measured using the measurement system shown in figure 9. If the envelope phase shift is φ_e, then the group delay can be calculated as

$$\varphi_e = W_m T_d$$

$$T_d = \frac{\varphi_e}{W_m} = \frac{\varphi_e}{(360° \times f_m)} \qquad \text{(A7)}$$

where f_m is the modulation frequency in Hz.

The group delay units are seconds. For $f_m = 2.778$ MHz, the envelope phase shift measured in degrees corresponds to group delay measured in nanoseconds.

Equation (A2) show that the group delay (T_d) measured is actually the average of the group delay at ($W_c - W_m$) and ($W_c + W_m$). This is the measurement "window" discussed in section 4.1, and is equal to ($W_c + W_m$) – ($W_c - W_m$) = $2W_m$.

ACCURACY CONSIDERATION

Several factors contribute to measurement uncertainties in the group delay measurement system shown in figure 9. The major ones are phase noise, modulation frequency inaccuracy, mismatch errors, and phase meter inaccuracy. These sources of error, and their effect on the overall measurement system accuracy, are discussed below.

Several sources of phase noise exist in the measurement system which can affect the accuracy of the measurement. The first source, which cannot be controlled, is the system under test. The SITE single channel transponder's local oscillators are specified as low phase noise devices, and spectral analysis indicates that the phase noise specifications are being met. No quantitative phase noise measurements are available.

The second source of phase noise is the modulation source. This noise does not affect the measurement since the noise is identical in the test channel and reference channels and is thus canceled in the phase meter measurement.

The third, and most significant, source of phase noise is from the CW signal source. If phase noise, φ_n, is added to the carrier signal in equation (A1), the result is

$$e_1(t) = E_1 (1 + M \sin W_m t) \sin (W_c t + \varphi_n) = E_1 \sin (W_c t + \varphi_n)$$

$$+ \left(\frac{M}{2}\right) E_1 \cos \left(W_c - W_m + \left(\frac{\varphi_n}{t}\right)\right) t + \frac{M}{2} E_1 \cos \left(W_c + W_m + \left(\frac{\varphi_n}{t}\right)\right) t \qquad \text{(A8)}$$

Carrying the phase noise term through the previous derivation (eqs. (A1) to (A5)), the result is

$$e_2(t) = E_2 \left\{ 1 + M \sin \left[\left(W_m + \left(\frac{\varphi_n}{t}\right)\right) t + \left(W_m + \left(\frac{\varphi_n}{t}\right)\right) T_d \right] \right\} \sin W_c(t + T_d) \qquad \text{(A9)}$$

14

The measured envelope phase shift becomes

$$\varphi_e = \left(W_m + \left(\frac{\varphi_n}{t}\right)\right)T_d \qquad \text{(A10)}$$

which now contains the phase noise term. As before, no quantitative measurement of the CW source phase noise is available. However, the effect of this noise on the measurement accuracy is lessened in the following ways. Choosing a synthesized signal source will provide the lowest available phase noise. The synthesizer chosen, Hewlett-Packard Model 8672A, has single-sideband phase noise of -78 dBc at 1 kHz for the frequencies being used (ref. 6), which is lower than any other available source. In addition, the computer control of the measurement allows multiple measurements to be made for a single test point, the results of which can be averaged to improve accuracy. Balancing the extra time required for multiple measurements against the improvement in accuracy, 20 measurements are made for each point during a typical group delay measurement. This results in an increase of the effective signal-to-noise ratio of 13 dB (refs. 9 and 10). These two techniques provide a measurement repeatability to within ±0.5 nsec.

The other three sources of group delay measurement uncertainty are more easily quantified. The first of these is modulation frequency inaccuracy. From equation (A7) the group delay measurement uncertainty resulting from modulation frequency inaccuracy is 0.0000375 percent per Hz of frequency error. In operating the group delay measurement setup, the modulation frequency is checked periodically with a frequency counter (EIP Microwave, Inc., Model 548). The specified maximum frequency error of this counter (ref. 7) is ±6.67 Hz, leading to a maximum group delay uncertainty of 0.00025 percent, which is negligible.

The mismatch errors which occur at the point of envelope detection will cause measurement uncertainty. Specifically, the mismatch differences between calibration and measurement can cause phase errors of several degrees (ref. 11). To keep these errors at a minimum, an isolator has been added to the envelope detector. Automatic network analyzer measurements indicate that the maximum output voltage standing-wave-ratio (VSWR) of these isolators is 1.2 to 1. A similar match is obtained at the system output, since identical isolators exist there. The modulator's VSWR has been measured at 1.2 to 1. Thus, the phase error limit is obtained by adding the mismatch error during calibration to the mismatch error during measurement. These errors are easily obtained from a mismatch error limits calculator (ref. 11). They are ±0.48° for calibration and ±0.48° for measurement, leading to an overall measurement uncertainty of ±0.96°, equal to 0.96 nsec.

The final major source of measurement uncertainty to be discussed is phase meter instrumentation error. This uncertainty is easily obtained from the manufacturer's specifications. For a single frequency measurement, the phase accuracy is given as ±1.5° (ref. 5).

The overall measurement uncertainty, including all of the quantifiable uncertainties discussed above, is approximately ±2.5 nsec. Comparisons of measurements made on a bandpass filter using the group delay measurement system with measurements made on the same filter with an automatic network analyzer show agreement to within 0.52 nsec in the passband.

15

It should be pointed out that the 2.5 nsec uncertainty generally holds across the entire measurement passband. When repeating measurements, it is found that the entire set of data points will shift by a few nanoseconds, while the shape of the curve (as measured by the largest peak-to-peak variation across the measurement passband) is constant to within ±0.5 nsec in approximately 90 percent of the cases observed. It is the group delay variation which is of greater importance, since a constant (flat) group delay, which introduces no additional distortion, can be added to any set of data without effect. Therefore, the ±0.5 nsec uncertainty figure, is a better figure of merit for the group delay measurement system.

A.2 CMSP INPUT DATA SET CONSTRUCTION

In this appendix, a brief description on the CMSP input data set construction used for the group delay distortion simulation is given.

Figure 14 shows a typical input data set, consisting of 23 lines. The title line, transmitter line, receiver line, filter line, and filter specification lines are required for the simulation and are described below.

The title line (beginning with TITL) identifies the input data set.

The transmitter line (beginning with XMTR) defines several of the simulation parameters. SMSK indicates the use of serial minimum-shift-keyed modulation. The second parameter, 220, indicates the data rate in symbols per sec. Note that 220 is used instead of 220×10^{-6}, to allow reasonable execution time for the simulation. This is allowable since all other simulation parameters have been similarly scaled. The third parameter is the frequency offset of the carrier frequency from the center of the simulation bandwidth, chosen to be 0.0. The fourth parameter is the number of samples per channel symbol, chosen to be 20. The fifth parameter is the number of symbols transmitted during the random data mode of the simulation, 1000. These last two parameters define the precision achieved for a given simulation, and must be balanced against execution time. The final parameter specified gives the frequency in transmission symbols of the printing of detection and tracking statistics.

The receiver line specifies the following parameters. The first three parameters, (1, 0.05, and 0.001) specify phase lock loop parameters, and the following three parameters (1, 0.4, and 0.001) specify the symbol timing loop. Standard recommended values have been chosen which approximate the operation of the modulators and demodulators developed for NASA. The next parameter defines the detector type as a matched filter filter-and-sample detector. The following parameter, 1.5, defines the bandwidth of the matched filter as 1.5 times the symbol period (which corresponds to the 300 MHz channel bandwidth for a 220 Mbps data rate). The final parameter is the receiver phase offset, which varies between simulations.

The filter card (beginning with FLT) first specifies the filter being used. In this case, it is filter 7 (in fig. 11) located after the satellite downlink. The second parameter is the ratio of filter bandwidth to information rate, chosen to be 1.8. This specifies a wider filter than was specified in the receiver, so that a completely flat channel amplitude response can be specified (no 3 dB rolloff occurs in the 330 MHz bandwidth). The third parameter, specifies the filter center frequency within the simulation bandwidth,

16

which is 0.0. The fourth parameter is used to specify the range of filter specifications in units of filter 3 dB bandwidths. The filter has 19 frequency samples. The center 11 samples comprise the 330 MHz band, the next sample on either side gives the 3 dB point of the filter, and the final three samples on either side give the rolloff to the 20 dB point. Thus, the fourth parameter is calculated to be 1.5. The fifth parameter simply deletes a phase response option not needed for the simulation. The sixth parameter gives the range of frequency response samples in terms of data rate, which is calculated to be 2.7. The next parameter is the number of filter samples, 19. The final parameter is a circular phase shift factor, which superimposes a linear phase shift on the specified phase points to ensure a causal filter. After trail and error, this parameter was determined to be 0.5.

The final 19 input data lines (beginning with SPEC) give the filter sampled frequency response. Each card contains two parameters. The first is the amplitude response (in normalized voltage, with 1.0 indicate zero loss). The second is the phase response, calculated from the desired group delay response, in radians.

REFERENCES

1. Laverghetta, T.S.: Handbook of Microwave Testing, Artech House, Dedham, MA, 1981.

2. Adam, S.F.: Microwave Theory and Applications, Prentice-Hall, 1969.

3. Ziemer, R.E.; and Tranter, W.H.: Principles of Communications, Houghton Mifflin Company, 1985.

4. Feher, K.: Digital Communications, Prentice-Hall, 1983.

5. 8405A Vector Voltmeter, Operating and Service Manual. Hewlett-Packard Co., Palo Alto, Ca, 1971, 1966c.

6. 8672A Synthesized Signal Generator, Operating and Service Manual. Hewlett-Packard Co., Palo Alto, Ca, 1980.

7. Models 545/548 Microwave Frequency Counters. EIP Microwave, Inc., San Jose, CA, 1980.

8. Swept-Frequency Group Delay Measurements. Application Note 77-4, Hewlett Packard Col, Palo Alto, CA, 1968.

9. Vifian, H.: Group Delay and AM-to-PM Measurement Techniques. Presented at the RF and Microwave Measurement Symposium and Exhibition, Hewlett-Packard Co., Palo Alto, CA, Mar. 1982.

10. McAllister, P.: Error Reduction in RF and Microwave Measurement. Microwave J., vol. 28, no. 10, Oct. 1985, pp. 131-142.

11. Adam, S.: Modern Microwave Measurements: Signal and Network Analysis (Course Notes). Technology Services Corp., Los Angeles, CA, 1983.

12. Amorosos, F.: The Badwidth of Digital Data Signals. IEEE Communications Magazine, vol. 18, no. 6, 1980, pp. 13-24.

13. Ziemer, R.E., and Ryan, C.R.: Minumum-Shift Keyed Modem Implementations for High Data Rates. IEEE Communications Magazine, vol. 21, no. 7, Oct. 1983, pp. 28-37.

14 Oetting, J.: A Comparison of Modulation Techniques for Digital Radio. IEEE Trans. Communications, vol. COM-27, no. 12, Dec. 1979, pp. 1752-1762.

15. Morais, D.; Sewerinson, A.; and Feher, K.: The Effects of the Amplitude and Delay Slope Components of Frequency Selective Fading on QPSK, Offset QPSK, and 8-PSK Systems. IEEE Trans. Communications, vol. Com-27, no. 12, Dec. 1979, pp. 1849-1853.

16. Channel Model Simulation Program, User's Manual. STI/E-TR-9035A, Stanford Telecommunications Institute, McLean, VA, Aug. 1983.

17. Weinberg, A.: The Effects of Transponder Imperfections on the Error Probability Performance of a Satellite Communication System. IEEE Trans. Communications, vol. COM-28, no. 6, June 1980, pp. 858-872.

18. Fujikawa, G.; and Kerczewski, R.J.: Performance of a Ka-Band Satellite System Under Variable Transmitted Signal Power conditions. To be presented at the IEEE MTT-S International Microwave Symposium, Las Vegas, NV, June 1987.

19. Kerczewski, R.J.; and Shalkhauser, K.A.: Automated Testing of Developmental Satellite Communications Systems and Subsystems. NASA TM-87070, 1985.

TABLE I. RESULTS OF SITE SATELLITE COMMUNICATIONS SYSTEM
SIMULATOR GROUP DELAY MEASUREMENTS

Power amplifier	Power Mode[a]	Operating point	Frequency band[b]	Matrix switch crosspoint[c]	Group delay variation[d]
GaAsFET	N/A	Saturation	A	4.3	2.98
			A	5.3	1.92
			B	6.3	1.37
			B	3.5	1.59
			C	5.5	9.07
			C	6.5	10.30
GaAsFET	N/A	1 dB compression point	A	3.6	5.46
			A	4.6	5.27
			B	6.6	9.57
			B	3.7	10.07
			C	4.7	20.86
			C	5.7	14.76
GaAsFET	N/A	Linear region	A	3.3	1.76
			A	4.5	1.59
			B	5.6	3.78
			B	6.7	1.71
			C	7.6	11.59
			C	3.3	5.24
Mean group delay variation, GaAsFET					6.60
Standard deviation, GaAsFET					5.31
TWTA	Low	Saturation	A	4.3	6.19
			A	5.3	6.95
			B	6.3	3.89
			B	3.5	4.34
			C	5.5	11.79
			C	6.5	11.52
TWTA	Low	1 db compression point	A	3.6	2.31
			A	4.6	2.34
			B	6.6	1.95
			B	3.7	2.15
			C	4.7	3.62
			C	5.7	4.04
TWTA	Low	Linear region	A	4.5	1.64
			A	5.6	1.55
			B	6.7	1.66
			B	7.6	1.24
			C	3.3	4.02
			C	4.5	9.97
Mean group delay variation, TWTA low mode					4.51
Standard deviation, TWTA low mode					3.33

[a]The TWTA operates in one of three power modes, with output power
   varying from 5 to 35 W.
[b]Frequency bands are as shown in figure 6.
[c]The crosspoint numbers indicate the connected matrix switch input
   and output ports, respectively.
[d]The maximum peak-to-peak group delay deviation, in nsec.

TABLE I. - Concluded.

Power amplifier	Power Mode[a]	Operating point	Frequency band[b]	Matrix switch crosspoint[c]	Group delay variation[d]
TWTA	Medium	Saturation	A	4.3	2.59
			A	5.3	2.20
			B	6.3	2.25
			B	3.5	1.86
			C	5.5	3.56
			C	6.5	2.94
TWTA	Medium	1 dB compression point	A	3.6	1.74
			A	4.6	1.77
			B	6.6	2.72
			B	3.7	2.86
			C	4.7	8.10
			C	5.7	6.65
TWTA	Medium	Linear region	A	5.6	1.90
			A	6.7	1.60
			B	7.6	1.62
			B	3.3	1.59
			C	4.5	9.14
			C	5.6	6.61
Mean group delay variation, TWTA medium mode					3.42
Standard deviation, TWTA medium mode					2.35
TWTA	High	Saturation	A	4.3	6.11
			A	5.3	5.65
			B	6.3	4.72
			B	3.5	5.02
			C	5.5	3.65
			C	6.5	4.10
TWTA	High	1 dB compression point	A	3.6	4.15
			A	4.6	3.98
			B	6.6	2.71
			B	3.7	2.74
			C	4.7	5.17
			C	5.7	4.62
TWTA	High	Linear region	A	6.7	1.85
			A	7.6	2.24
			B	3.3	2.32
			B	4.5	2.22
			C	5.6	4.02
			C	6.7	9.97
Mean group delay variation, TWTA high mode					3.78
Standard deviation, TWTA high mode					1.23
Mean group delay variation, all cases					4.72
Standard deviation, all cases					3.70

[a]The TWTA operates in one of three power modes, with output power varying from 5 to 35 W.
[b]Frequency bands are as shown in figure 6.
[c]The crosspoint numbers indicate the connected matrix switch input and output ports, respectively.
[d]The maximum peak-to-peak group deviation, in nsec.

20

TABLE II. RESULTS OF SITE SATELLITE COMMUNICATIONS SYSTEM SIMULATOR BIT ERROR RATE MEASUREMENTS

Power amplifier	Power Mode[a]	Operating point	Frequency band[b]	Matrix switch crosspoint[c]	E_b/N_0 at BER $= 5 \times 10^{-7}$ [d]
TWTA	Low	Saturation	A	4.3	0.80
			A	5.3	1.00
			B	6.3	.80
			B	3.5	.98
			C	5.5	2.43
			C	6.5	3.57
TWTA	Low	1 dB compression point	A	3.6	1.26
			A	4.6	1.32
			B	6.6	.79
			B	3.7	.95
			C	4.7	3.49
			C	5.7	3.73
TWTA	Low	Linear region	A	4.5	.94
			A	5.6	1.58
			B	6.7	1.30
			B	7.6	1.46
			C	3.3	5.70
			C	4.5	5.01
Mean E_b/N_0 degradation, TWTA low mode					2.06
Standard deviation, TWTA low mode					1.51
TWTA	Medium	Saturation	A	4.3	1.08
			A	5.3	1.15
			B	6.3	.85
			B	3.5	.87
			C	5.5	2.10
			C	6.5	3.13
TWTA	Medium	1 dB compression point	A	3.6	1.59
			A	4.6	1.87
			B	6.6	.97
			B	3.7	1.26
			C	4.7	5.09
			C	5.7	5.78
TWTA	Low	Linear region	A	5.6	3.67
			A	6.7	2.07
			B	7.6	1.76
			B	3.3	2.10
			C	4.5	6.40
			C	5.6	7.15
Mean E_b/N_0 degradation, TWTA medium mode					2.72
Standard deviation, TWTA medium mode					1.98

[a]The TWTA operates in one of three power modes, with output power varying from 5 to 35 W.
[b]Frequency bands are as shown in figure 6.
[c]The crosspoint numbers indicate the connected matrix switch input and output ports, respectively.
[d]The additional E_b/N_0 required to maintain a bit error rate of 5×10^{-7} as measured from the theoretical SMSK curve.

21

TABLE II. – Concluded.

Power amplifier	Power Mode[a]	Operating point	Frequency band[b]	Matrix switch crosspoint[c]	E_b/N_0 at BER = 5×10^{-7} [d]
TWTA	High	Saturation	A	4.3	2.59
			A	5.3	2.20
			B	6.3	2.25
			B	3.5	1.86
			C	5.5	3.56
			C	6.5	2.94
TWTA	High	1 dB compression point	A	3.6	1.74
			A	4.6	1.77
			B	6.6	2.72
			B	3.7	2.86
			C	4.7	8.10
			C	5.7	6.65
TWTA	High	Linear region	A	6.7	2.19
			A	7.6	3.41
			B	3.3	1.80
			B	4.5	2.31
			C	5.6	1.36
			C	6.7	2.15
Mean E_b/N_0 degradation, TWTA high mode					2.71
Standard deviation, TWTA high mode					1.21
Mean E_b/N_0 degradation, all cases					2.50
Standard deviation, all cases					1.63

[a]The TWTA operates in one of three power modes, with output power varying from 5 to 35 W.
[b]Frequency bands are as shown in figure 6.
[c]The crosspoint numbers indicate the connected matrix switch input and output ports, respectively.
[d]The additional E_b/N_0 required to maintain a bit error rate of 5×10^{-7} as measured from the theoretical SMSK curve.

MODULATOR

DEMODULATOR
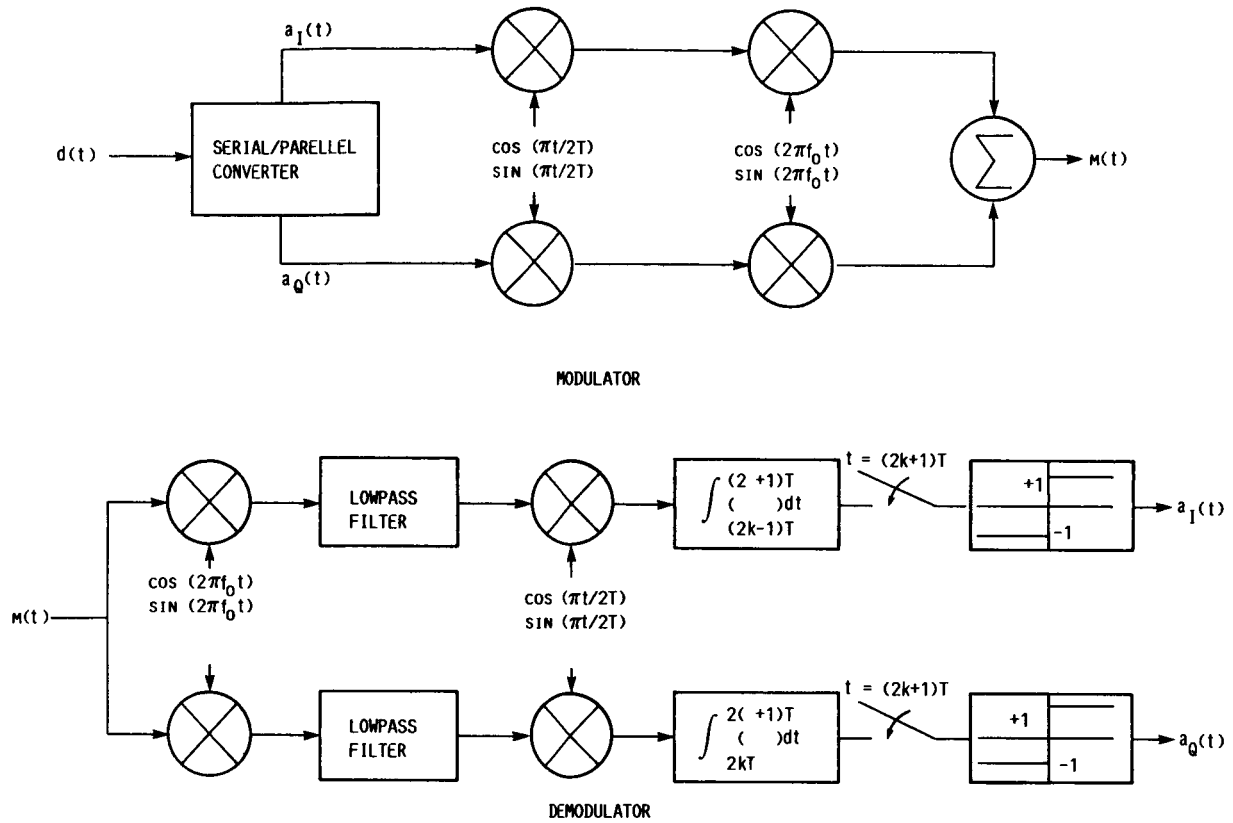
FIGURE 1. - PARALLEL MSK IMPLEMENTATION (FROM REF. 13).
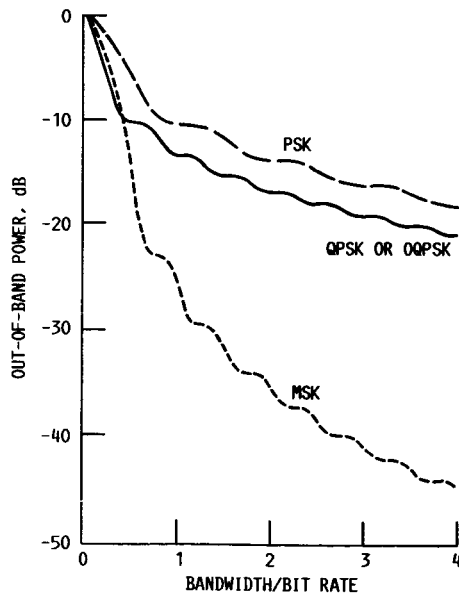
FIGURE 2. - FRACTIONAL OUT-OF-BAND POWER
FOR PSK, QPSK, OQPSK, AND MSK (REF. 3).

MODULATOR
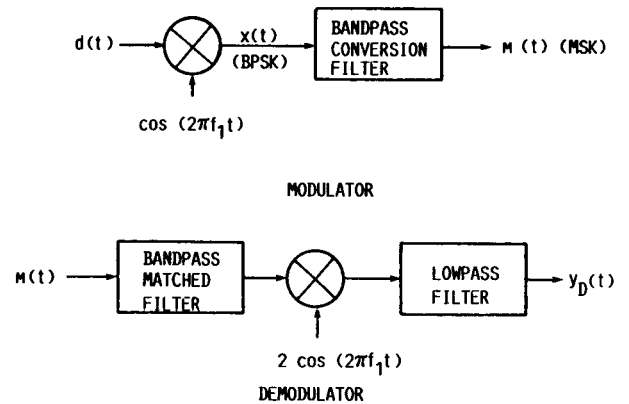
DEMODULATOR

FIGURE 3. - SERIAL MSK IMPLEMENTATION (FROM REF. 13).

23
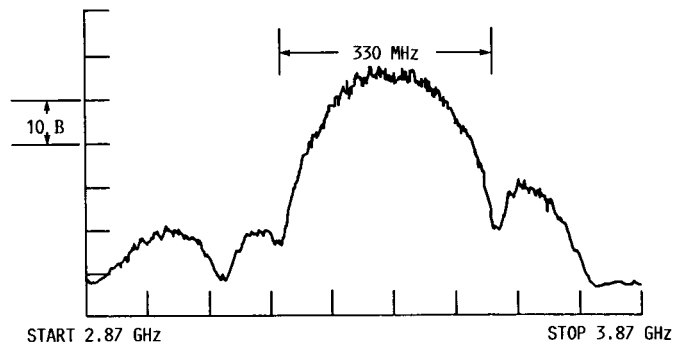
FIGURE 4. - SMSK MODULATION SPECTRUM AT A DATA RATE OF
220 MBPS.
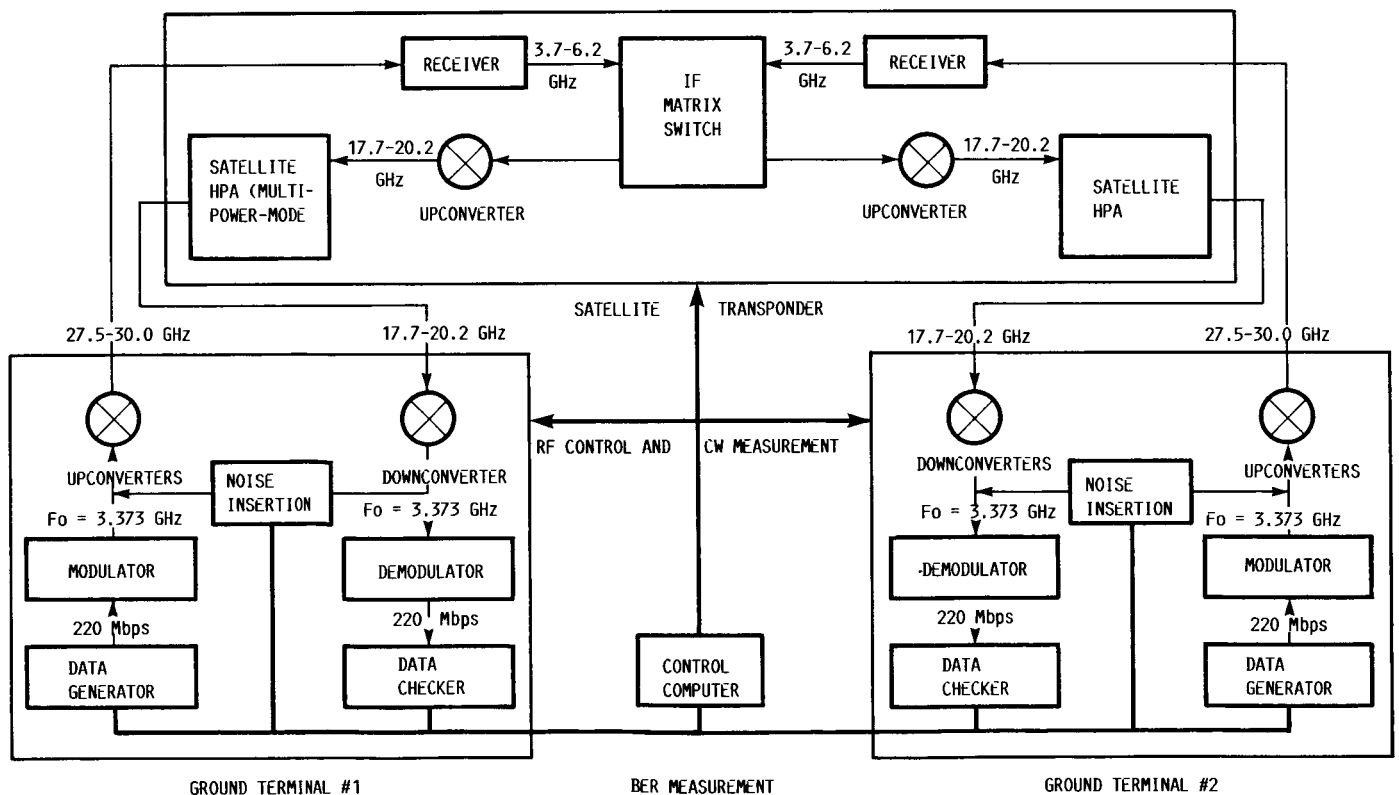
FIGURE 5. - SITE SATELLITE COMMUNICATION SYSTEM SIMULATOR.

24
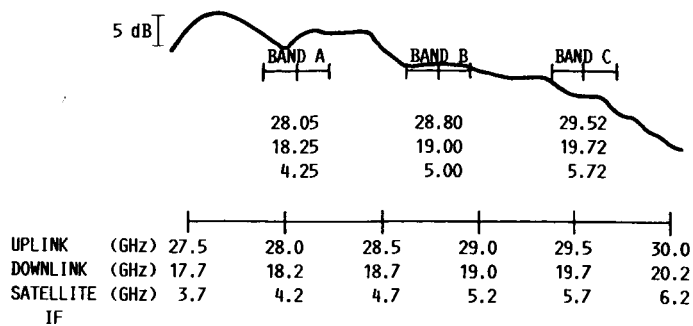
FIGURE 6. - SPECTRAL LOCATION OF TEST BANDS (APPROXIMATE LINEAR FRE-
QUENCY RESPONSE IS SHOWN).

		BAND A		BAND B		BAND C	
		28.05		28.80		29.52	
		18.25		19.00		19.72	
		4.25		5.00		5.72	
UPLINK	(GHz)	27.5	28.0	28.5	29.0	29.5	30.0
DOWNLINK	(GHz)	17.7	18.2	18.7	19.0	19.7	20.2
SATELLITE IF	(GHz)	3.7	4.2	4.7	5.2	5.7	6.2
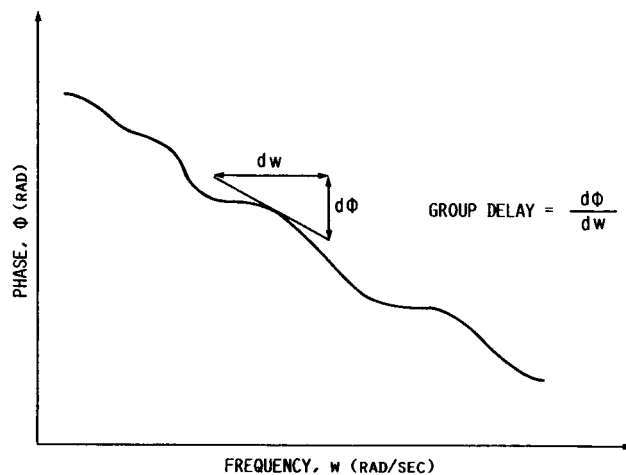
GROUP DELAY = $\dfrac{d\Phi}{dw}$

FIGURE 7. - DEFINITION OF GROUP DELAY.

f_C = CARRIER FREQUENCY

f_M = MODULATION FREQUENCY
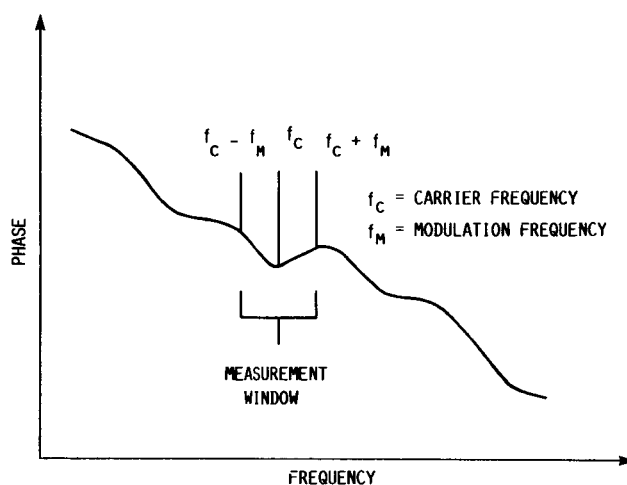
FIGURE 8. - DEFINITION OF THE GROUP DELAY MEASUREMENT WINDOW.

1 DEG PHASE SHIFT = 1 NSEC GROUP DELAY
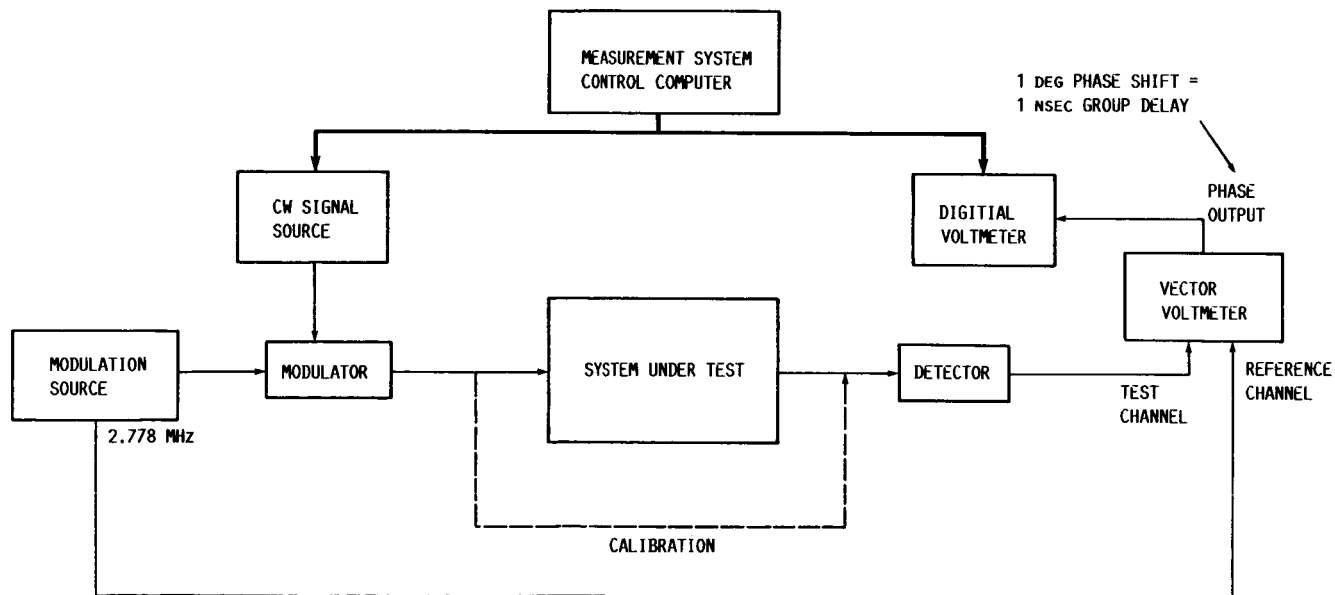
FIGURE 9. - GROUP DELAY MEASUREMENT SETUP.

25
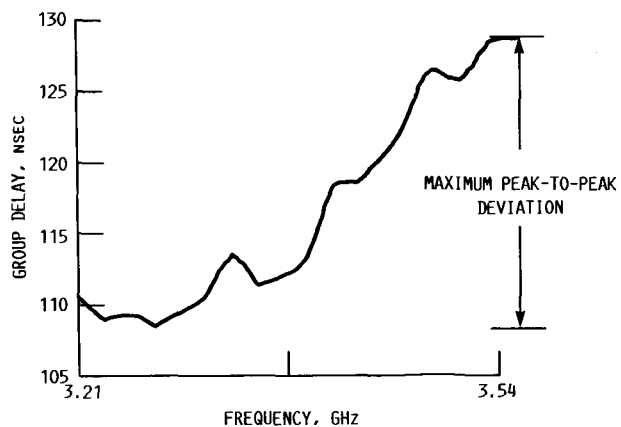
FIGURE 10. - TYPICAL GROUP DELAY MEASUREMENT
OUTPUT PLOT.
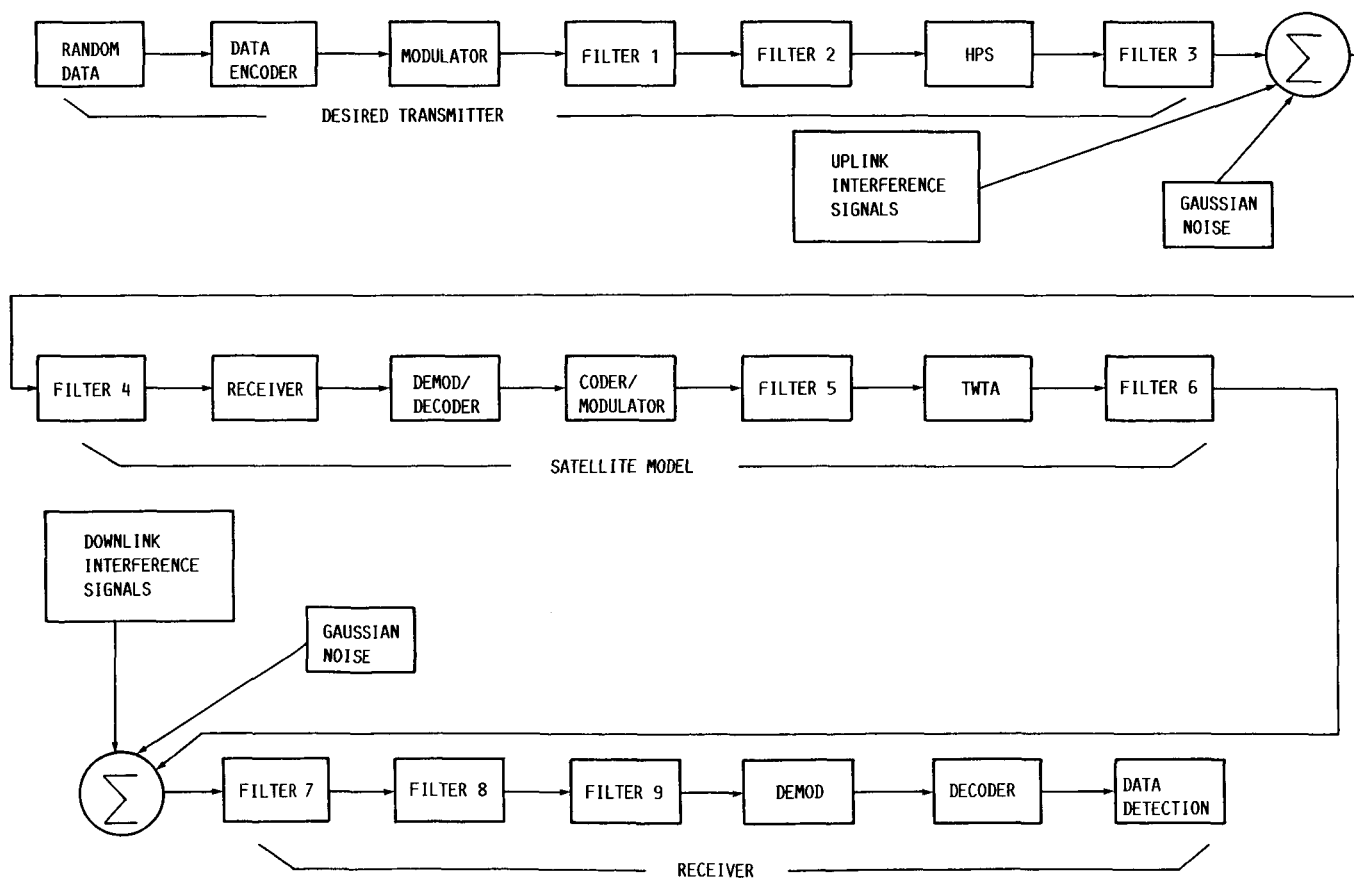
FIGURE 11. - CMSP SIMULATION CONFIGURATION.
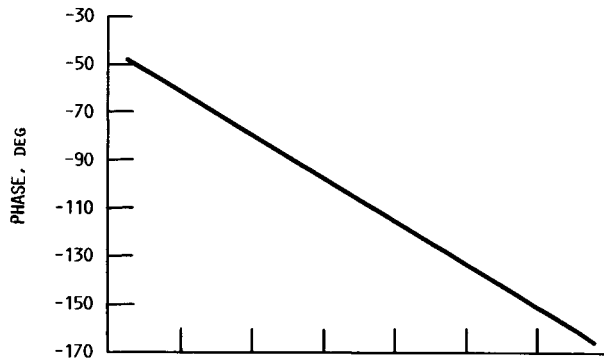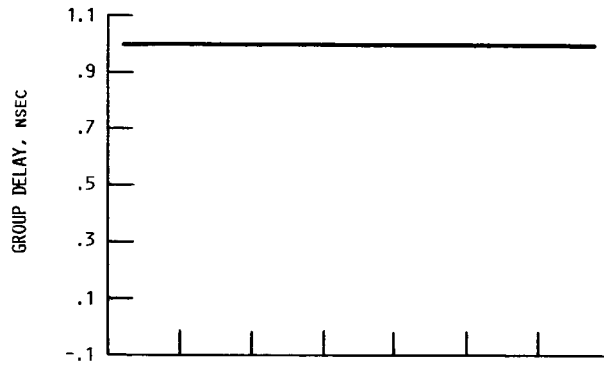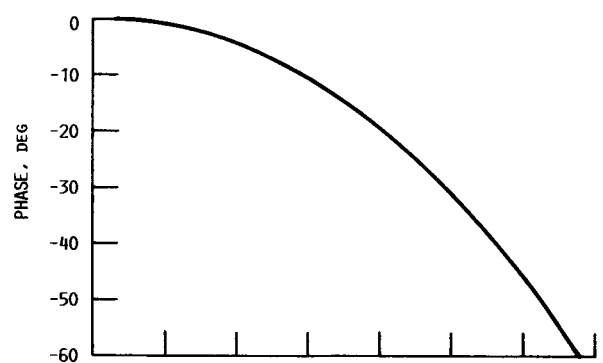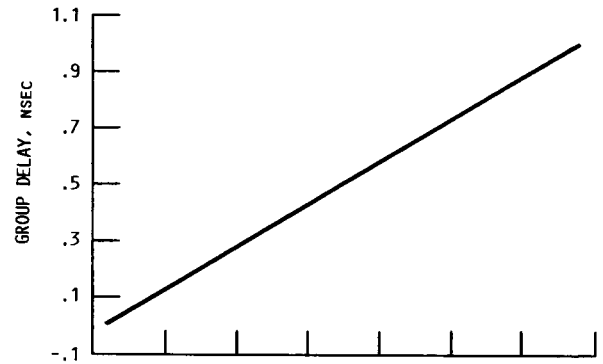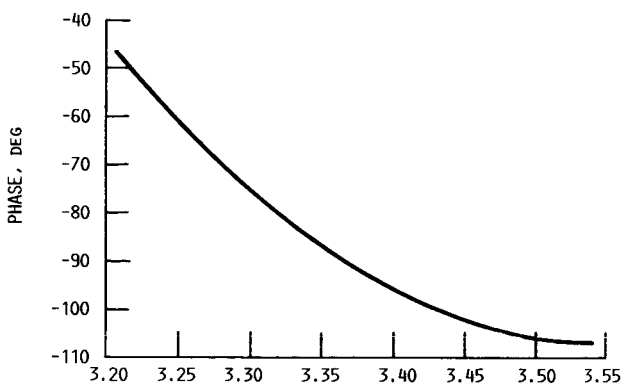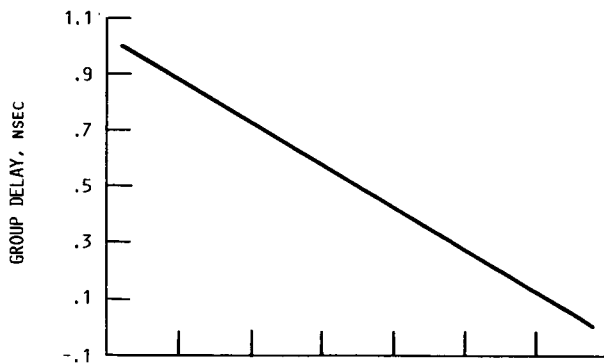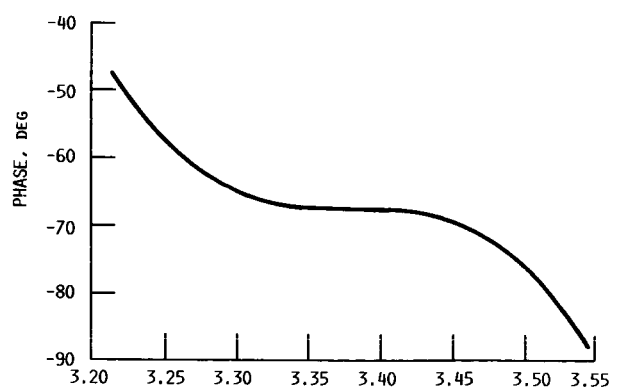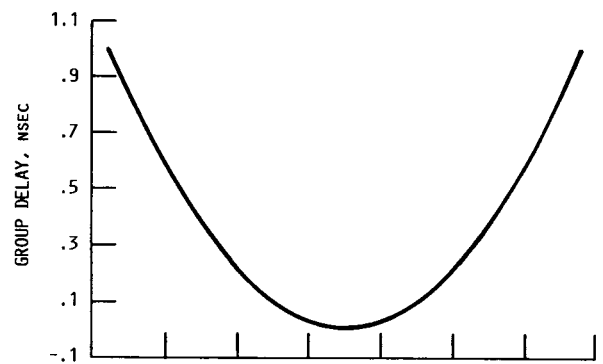
FIGURE 12. - GROUP DELAY PROFILES AND CORRESPONDING PHASE RESPONSES FOR CMSP GROUP DELAY DISTORTION SIMULATIONS.

27
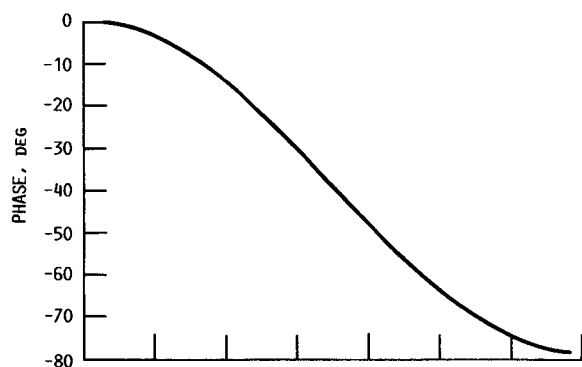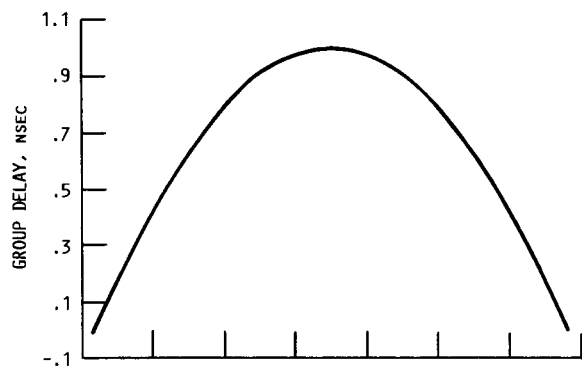
(E) INV PARABOLIC, CONVEX.
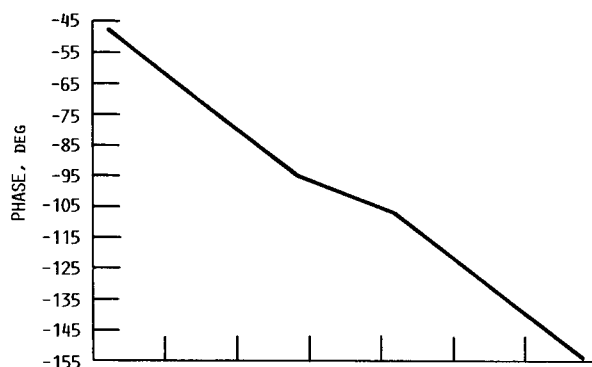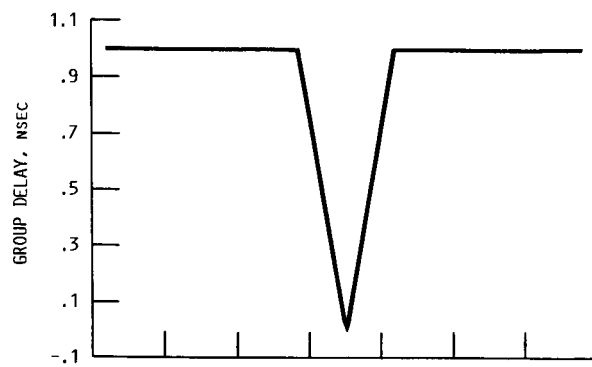
(G) CENTER SPIKE, NEGATIVE.
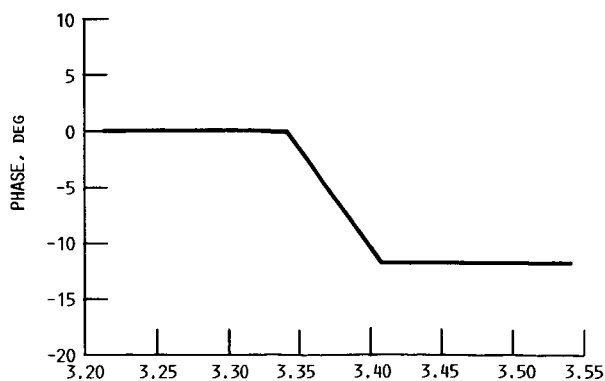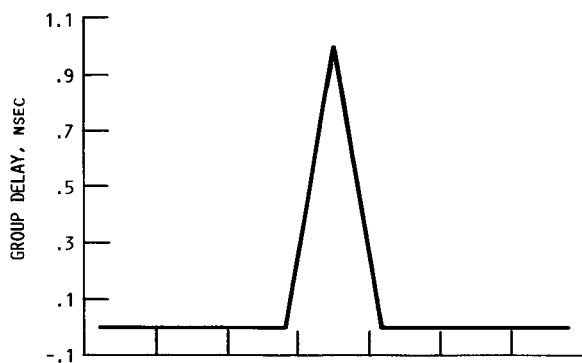
(F) CENTER SPIKE, POSITIVE.
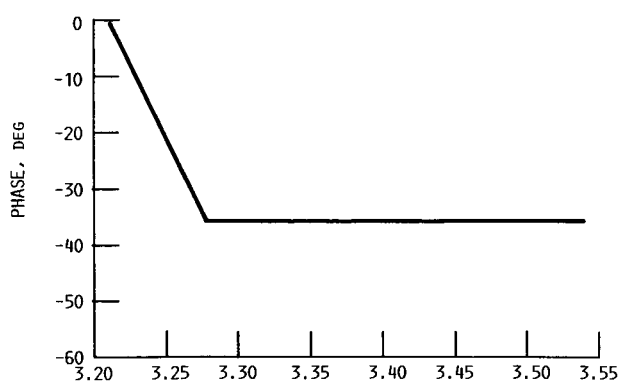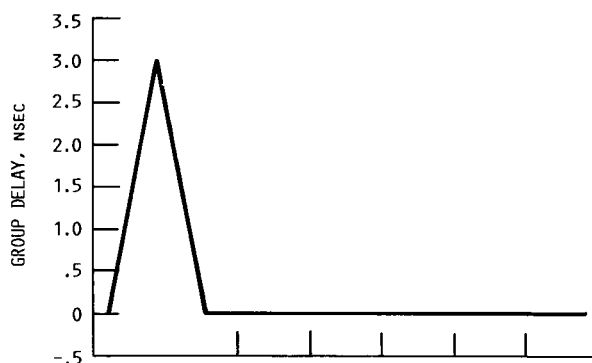
(H) VARIABLE SPIKE, POSITIVE.

FREQUENCY, GHz

FIGURE 12. – CONTINUED.

28
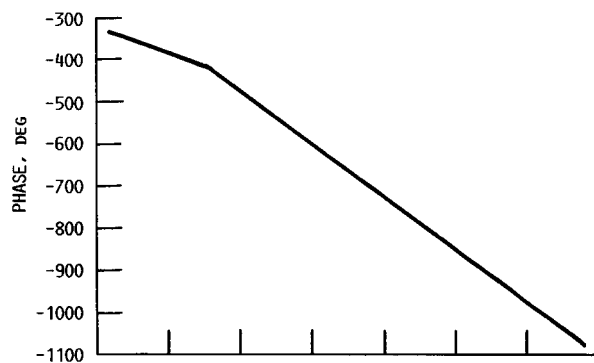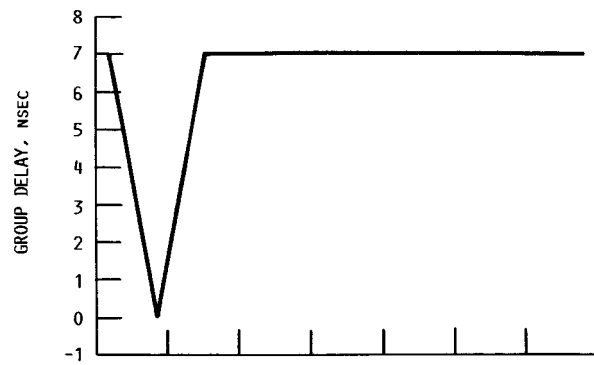
(I)VARIABLE SPIKE, NEGATIVE.
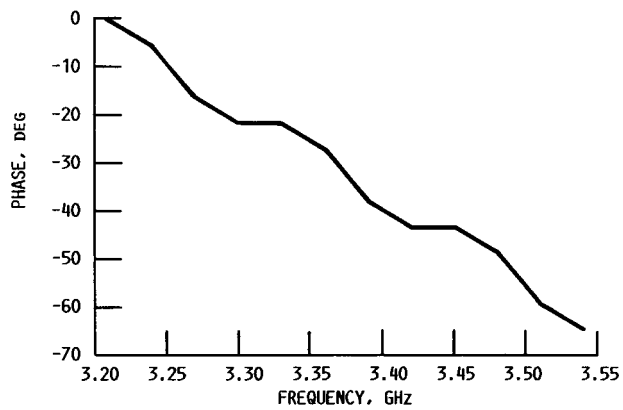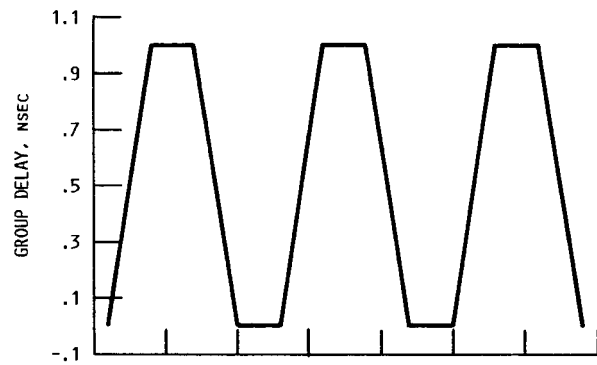
(K) PERIODIC RIPPLE.
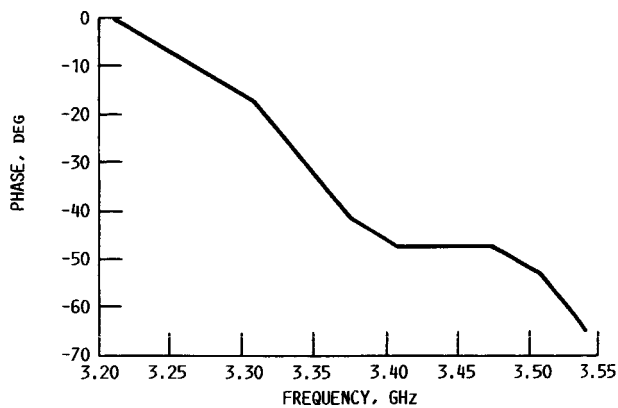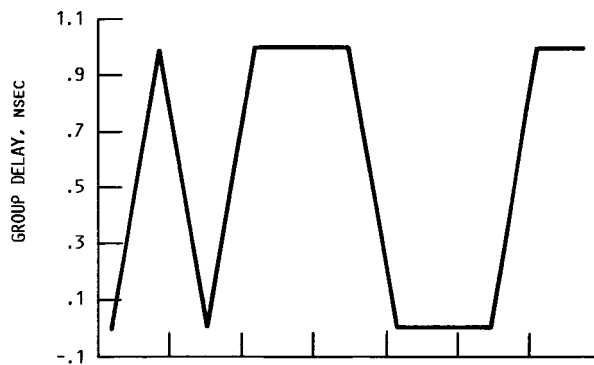
(J) NONPERIODIC RIPPLE.

FIGURE 12. - CONCLUDED.

29
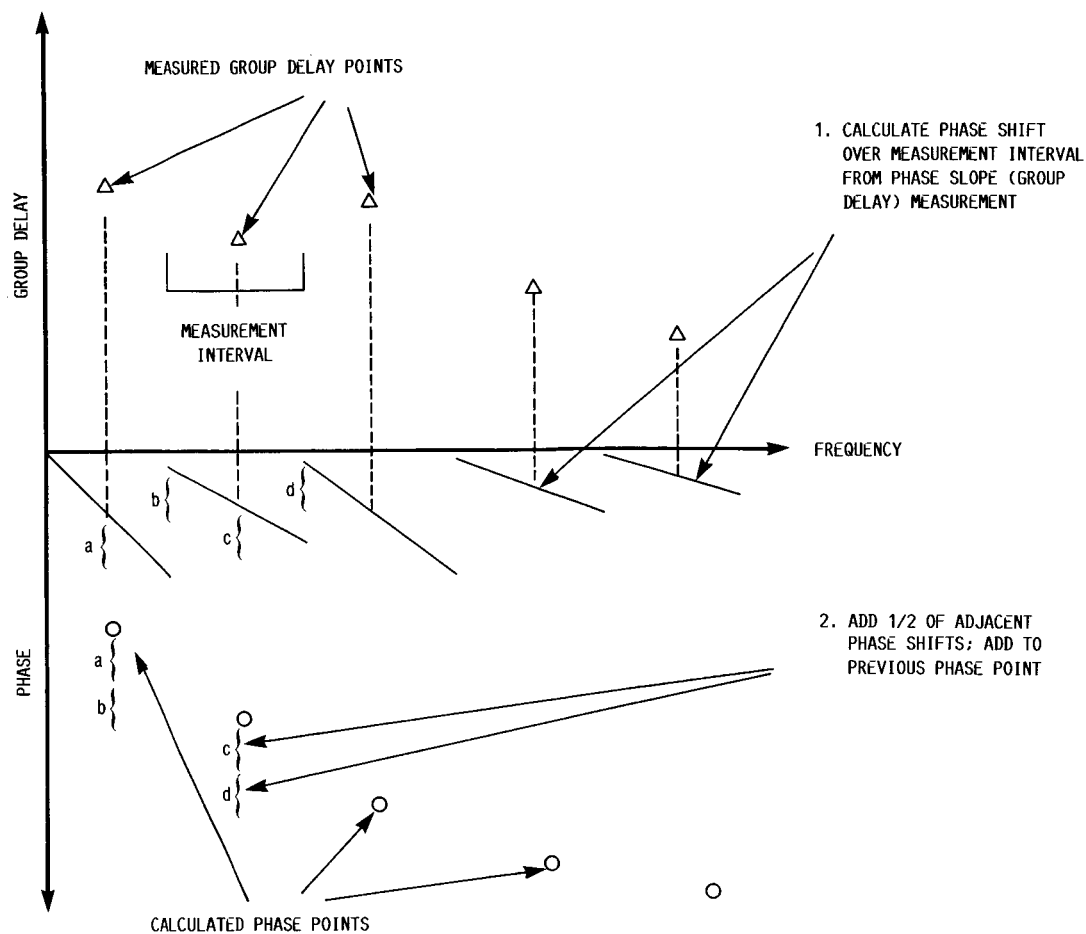
FIGURE 13. - INTEGRATION OF GROUP DELAY TO OBTAIN PHASE REPONSE.

```
TITL GROUP DELAY SET 2    Q8 - BAND 4 - MED MODE - XPT 3-3
XMTR SMSK 220          0.0          20 1000        100
RCVR 1 0.5     .001    1 0.4   .001   2 1.5   0.36
FLT7 1.8    0.0                 1.5      0 2.7   19                         0.5
SPEC 0.1               0.0
SPEC 0.3162           -0.021
SPEC 0.5012           -0.041
SPEC 0.7071           -0.062
SPEC 1.0              -0.083
SPEC 1.0              -0.093
SPEC 1.0              -0.104
SPEC 1.0              -0.218
SPEC 1.0              -0.456
SPEC 1.0              -0.705
SPEC 1.0              -1.026
SPEC 1.0              -1.389
SPEC 1.0              -1.794
SPEC 1.0              -2.348
SPEC 1.0              -3.058
SPEC 0.7071           -3.867
SPEC 0.5012           -4.676
SPEC 0.3162           -5.484
SPEC 0.1              -6.293
```

FIGURE 14. - TYPICAL CMSP INPUT DATA SET FOR GROUP DELAY DISTORTION SIMULATIONS.

30

```
GROUP DELAY SET 2    B10
  EBNO
   1.00      0.5628E-01      0.9390E-01
   2.00      0.3751E-01      0.7343E-01
   3.00      0.2288E-01      0.5565E-01
   4.00      0.1250E-01      0.4078E-01
   5.00      0.5954E-02      0.2884E-01
   6.00      0.2388E-02      0.1959E-01
   7.00      0.7727E-03      0.1271E-01
   8.00      0.1909E-03      0.7772E-02
   9.00      0.3363E-04      0.4399E-02
  10.00      0.3872E-05      0.2244E-02
  11.00      0.2613E-06      0.9982E-03
  12.00      0.9006E-08      0.3728E-03
  13.00      0.1333E-09      0.1119E-03
  14.00      0.6811E-12      0.2567E-04
  15.00      0.9124E-15      0.4240E-05
  16.00      0.2268E-18      0.4689E-06
  17.00      0.6759E-23      0.3180E-07
  18.00      0.1396E-28      0.1186E-08
  19.00      0.1001E-35      0.2123E-10
  20.00      0.1044E-44      0.1533E-12
```

FIGURE 15. - TYPICAL CMSP OUTPUT BER VERSUS Eb/No TABLE.

FLAT GROUP DELAY (EXPERIMENT CONTROL)
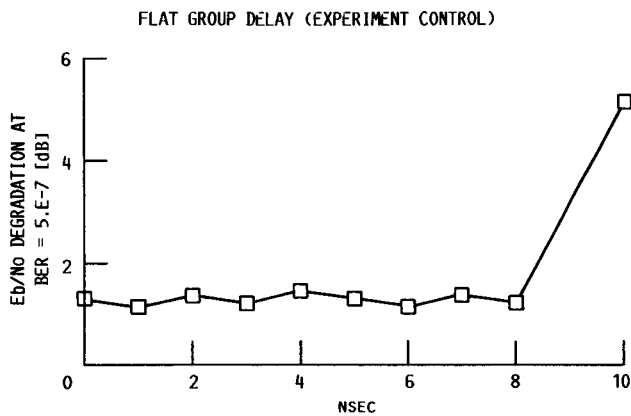
FIGURE 17. - Eb/No DEGRADATION DUE TO FLAT GROUP DELAY FROM
CMSP SIMULATIONS.

FIGURE 16. - BER VERSUS Eb/No CURVES FOR POSITIVE SLOPE
GROUP DELAY DISTORTION SIMULATION FROM CMSP.

GROUP DELAY DISTORTION - LINEAR SLOPE

FIGURE 18. - Eb/No DEGRADATION DUE TO LINEAR SLOPE GROUP
DELAY DISTORTION FROM CMSP SIMULATIONS.

GROUP DELAY DISTORTION - PARABOLIC
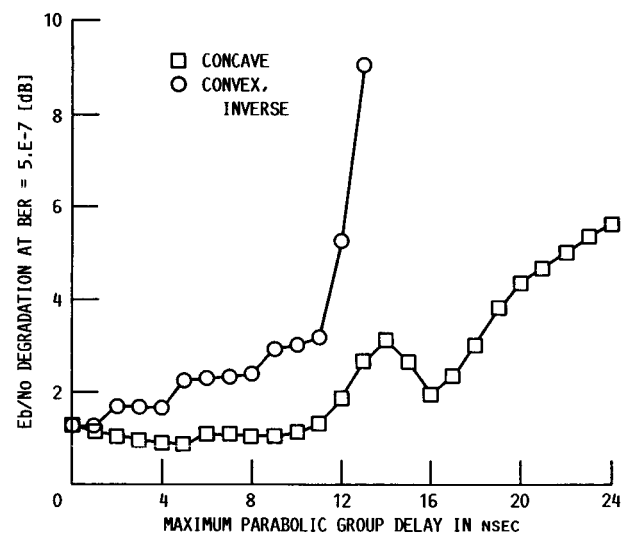
FIGURE 19. - Eb/No DEGRADATION DUE TO PARABOLIC GROUP DE-
LAY DISTORTION FROM CMSP SIMULATIONS.

31

GROUP DELAY DISTORTION - CENTER SPIKE

GROUP DELAY DISTORTION - SPIKE
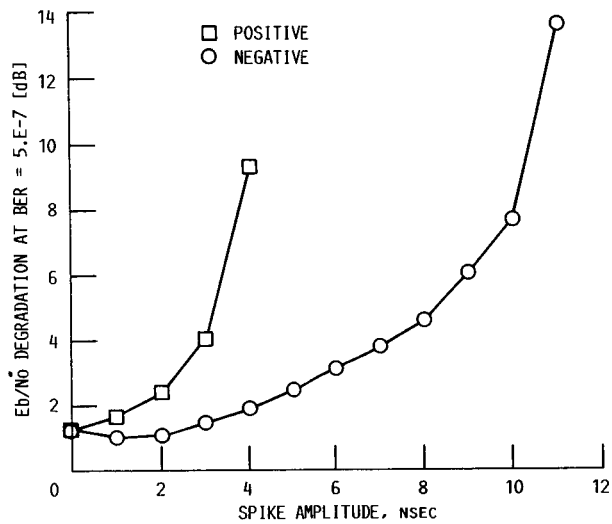
FIGURE 20. - Eb/No DEGRADATION DUE TO A GROUP DELAY SPIKE LOCATED AT THE BAND CENTER FROM CMSP SIMULATIONS.
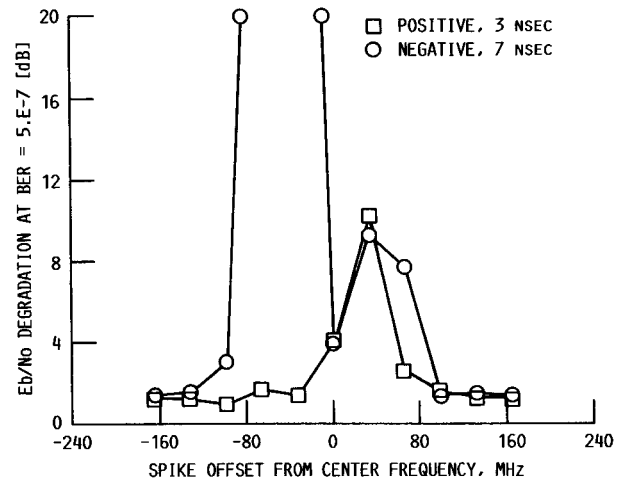
FIGURE 21. - Eb/No DEGRADATION DUE TO GROUP DELAY SPIKES AT VARIOUS OFFSETS FROM THE BAND CENTER FROM CMSP SIMULATIONS.

GROUP DELAY RIPPLE

Eb/No VERSUS GROUP DELAY
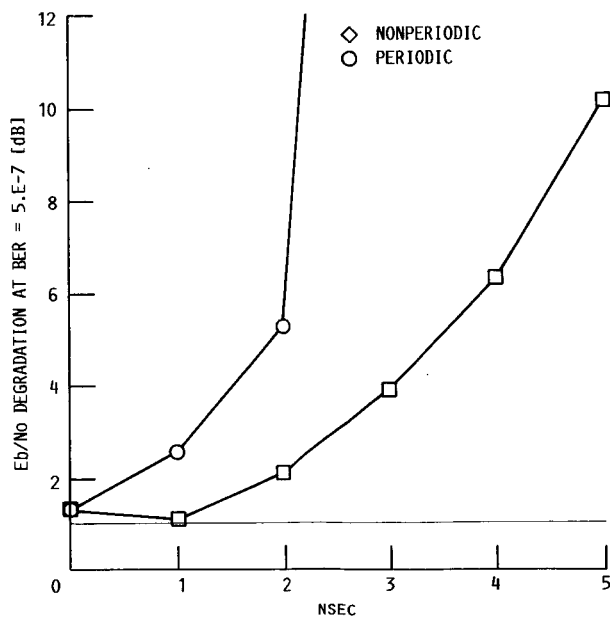
FIGURE 22. - Eb/No DEGRADATION DUE TO GROUP DELAY RIPPLE DISTORTION FROM CMSP SIMULATIONS.
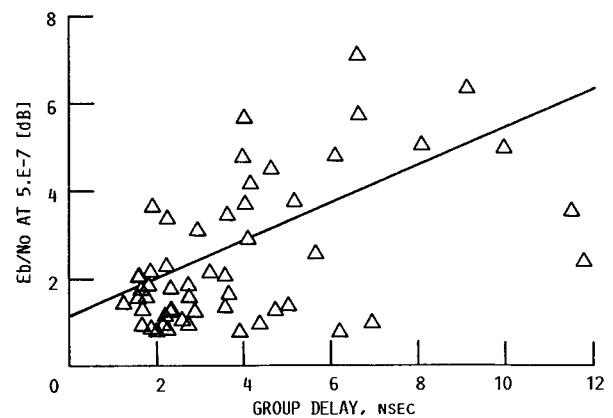
FIGURE 23. - MEASURED Eb/No DEGRADATION PLOTTED AGAINST MEASURED GROUP DELAY VARIATION.

32
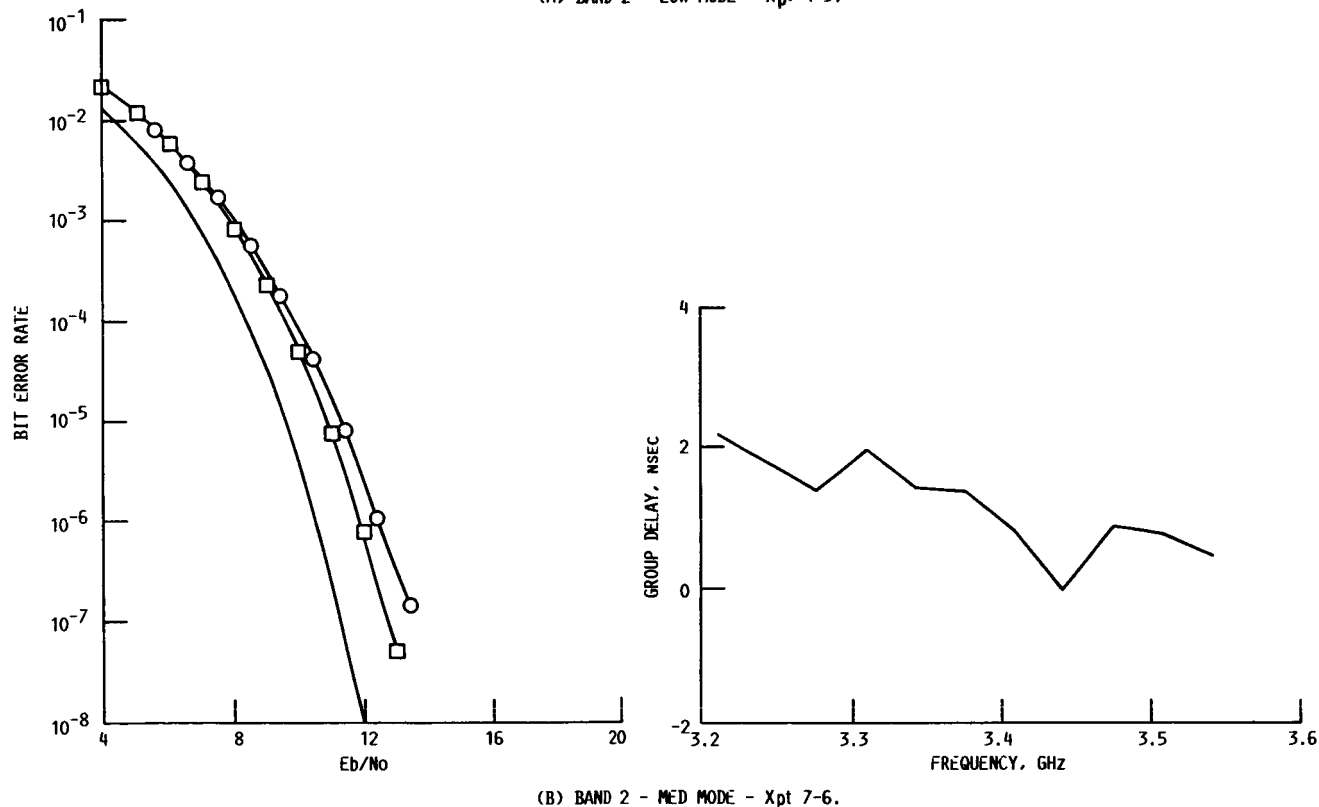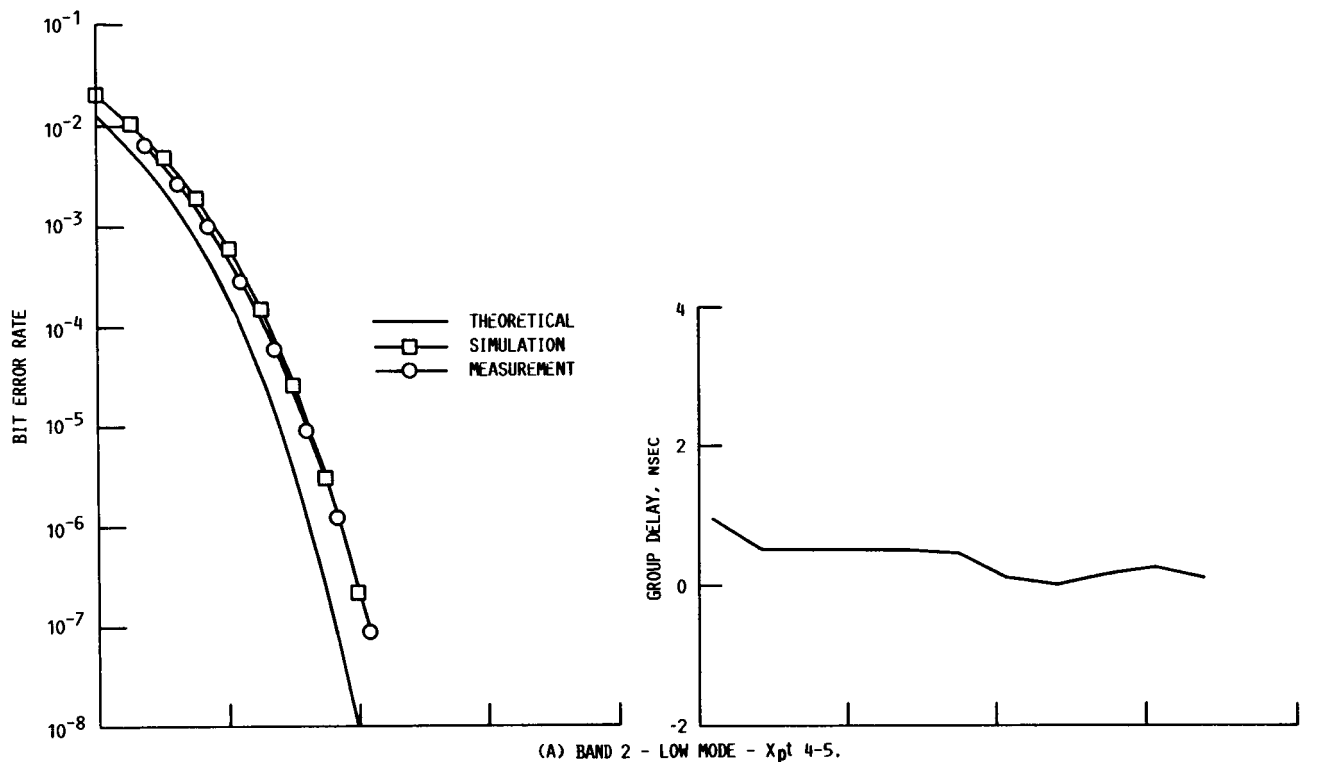
FIGURE 24. - CMSP PREDICTED BER RESPONSE AND MEASURED BER RESPONSE FOR TEN CASES.   MEASURED GROUP DELAY RESPONSES ARE SHOWN.
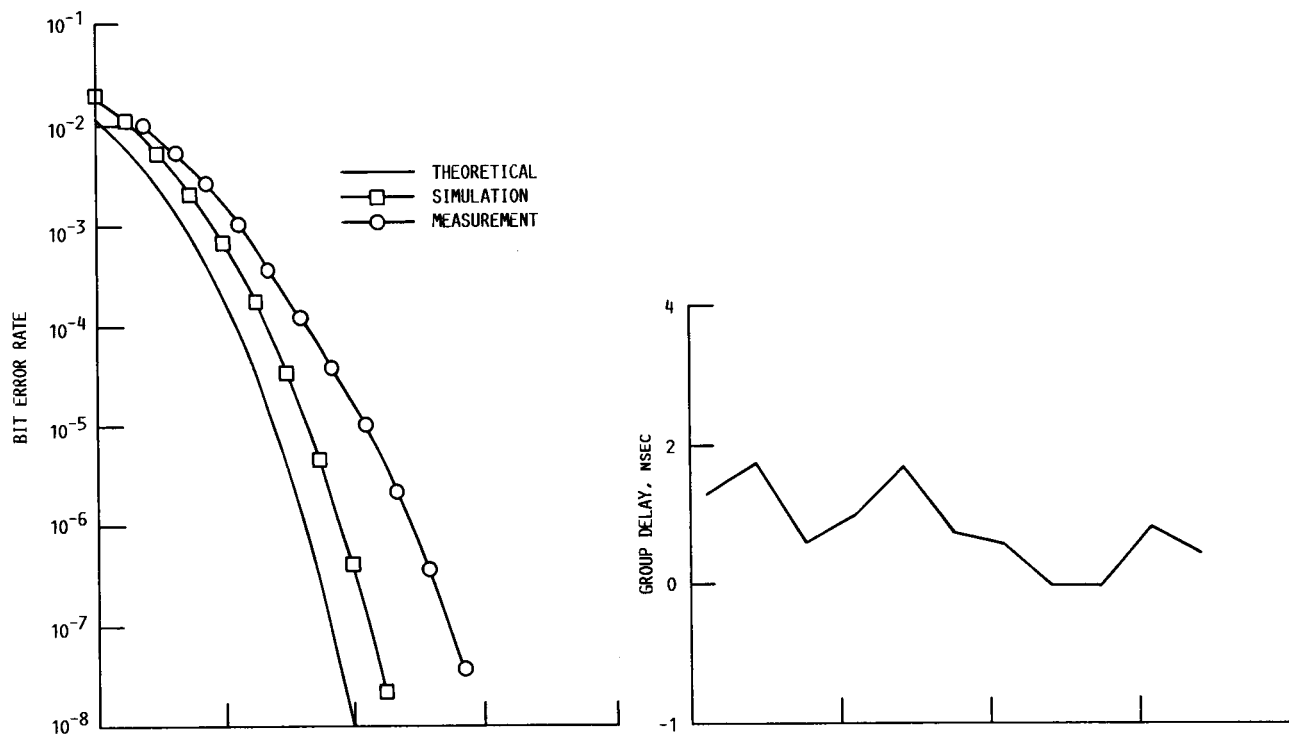
(C) BAND 3 - LOW MODE - Xpt 7-6.
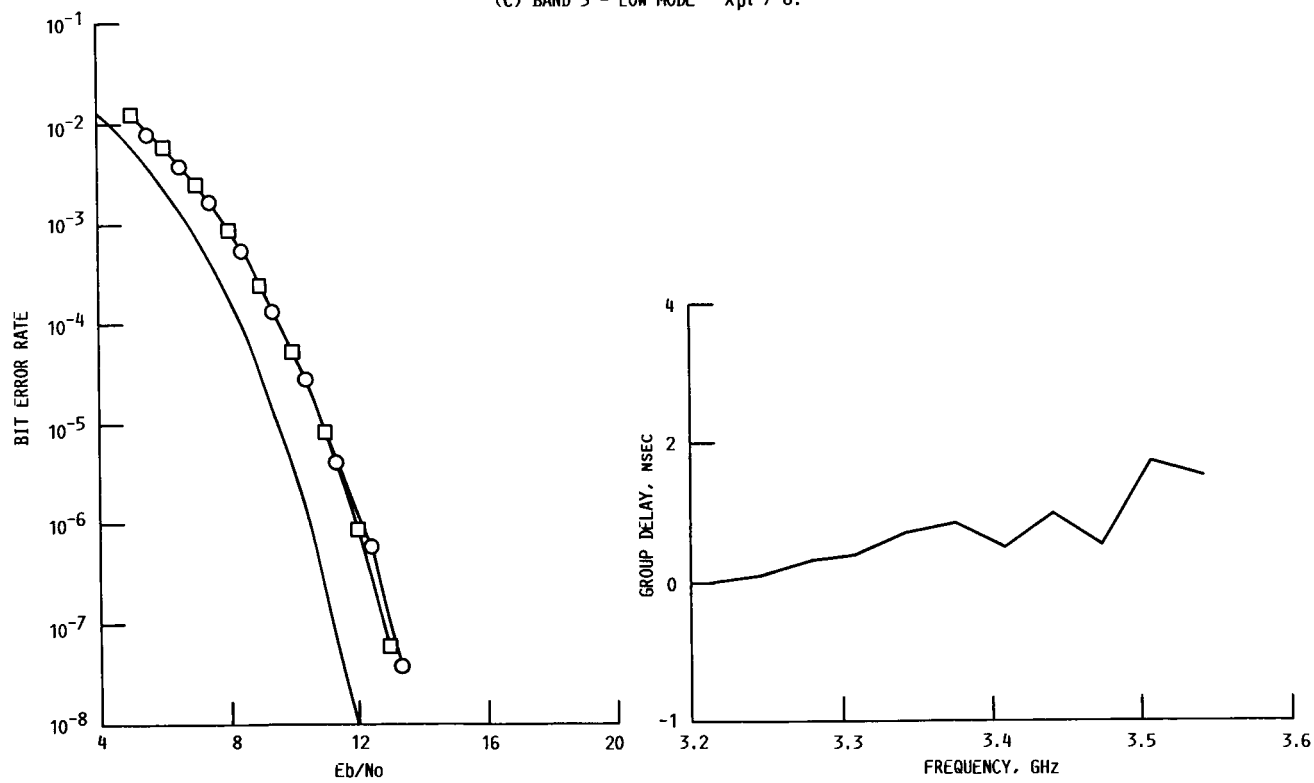
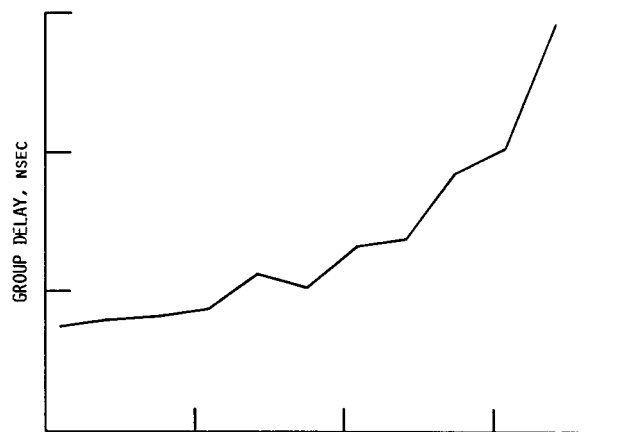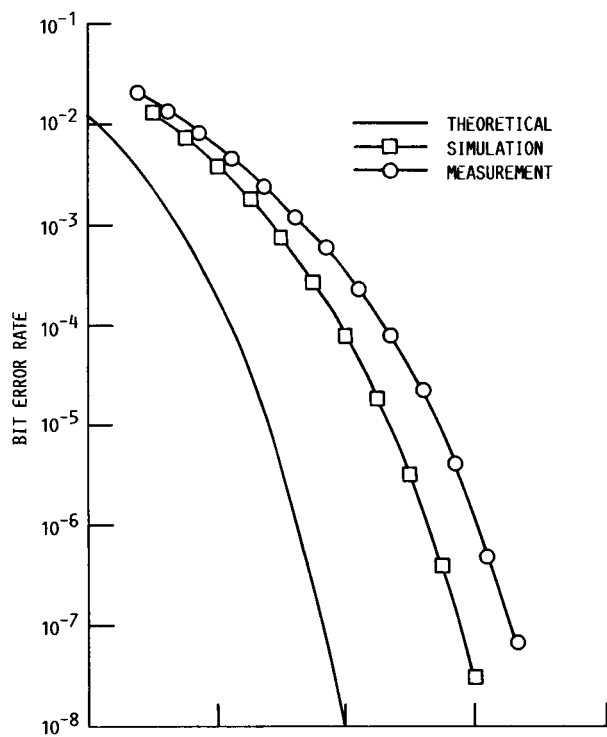(D) BAND 3 - LOW MODE - Xpt 4-5.
FIGURE 24. - CONTINUED.
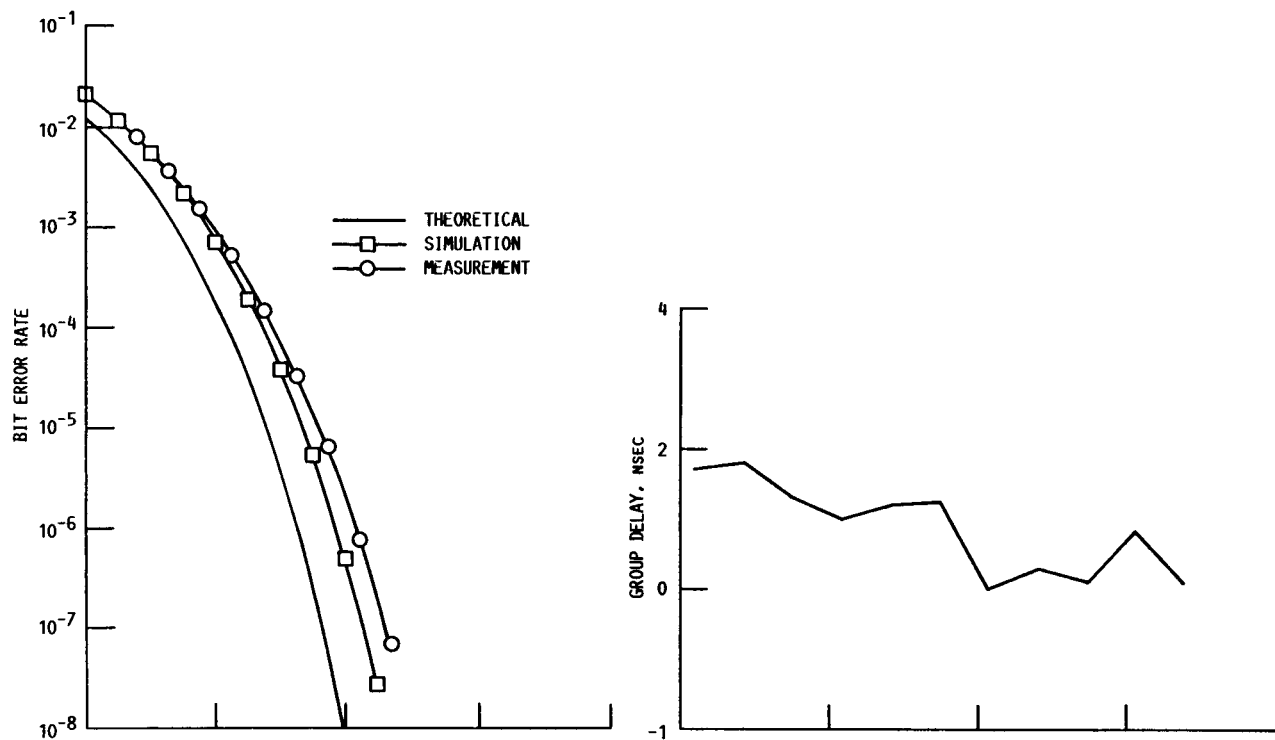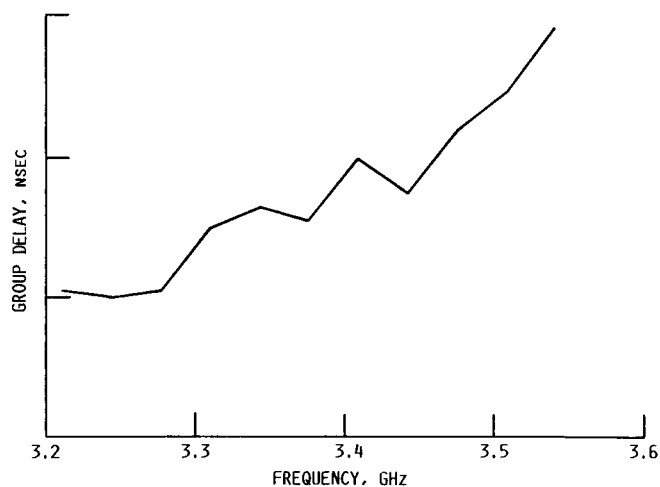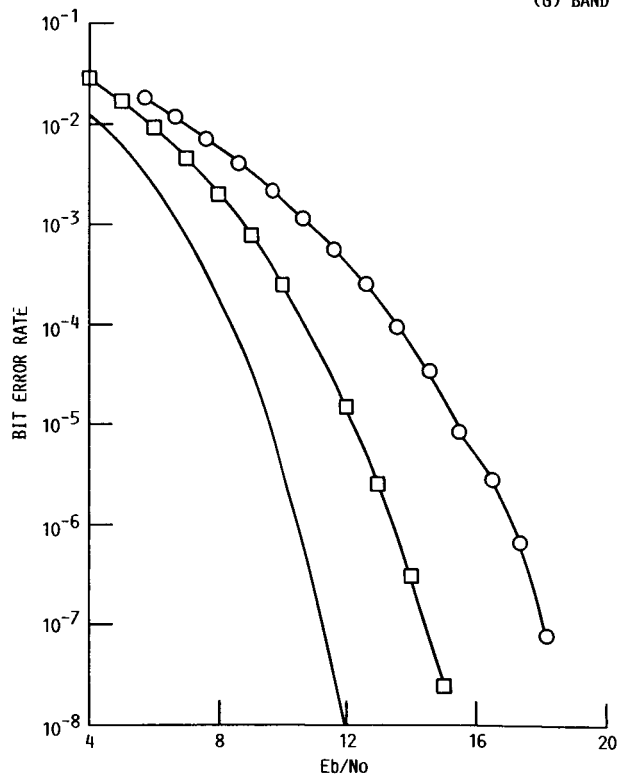
(E) BAND 3 - MED MODE - Xpt 5-6.
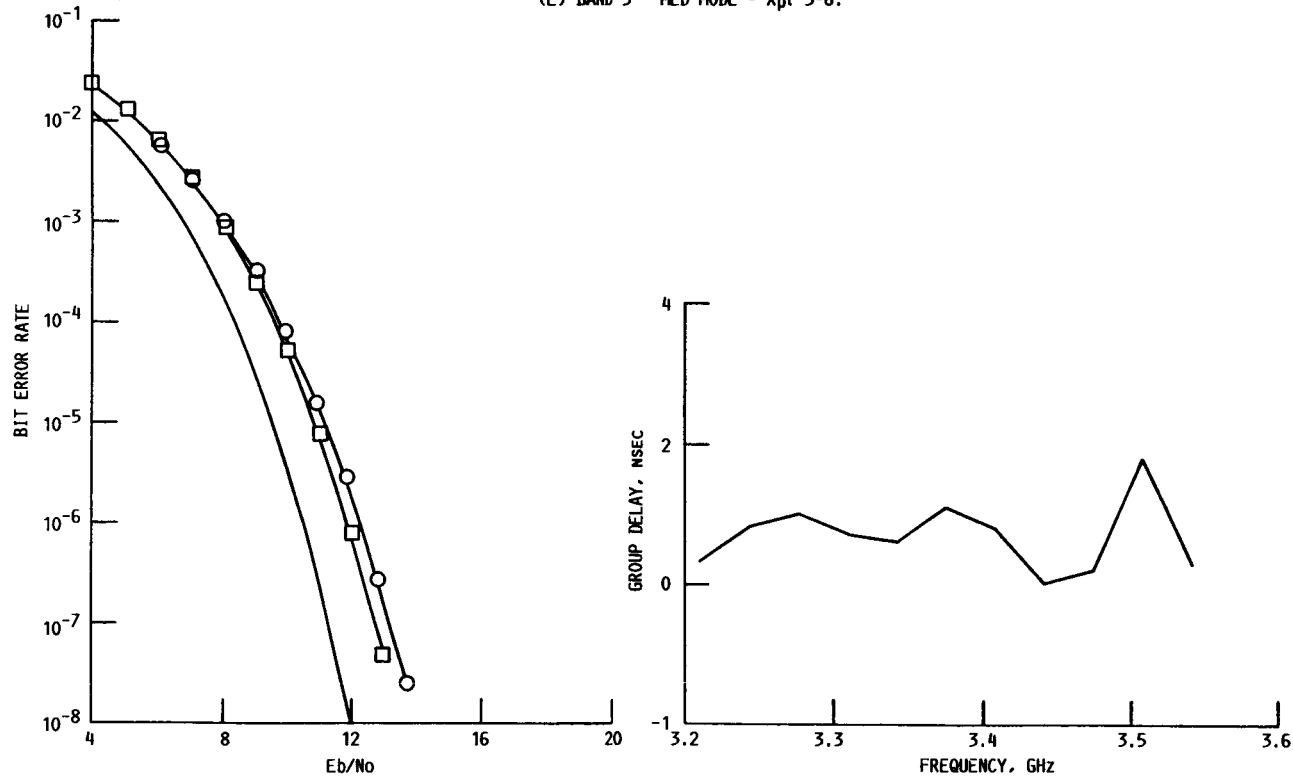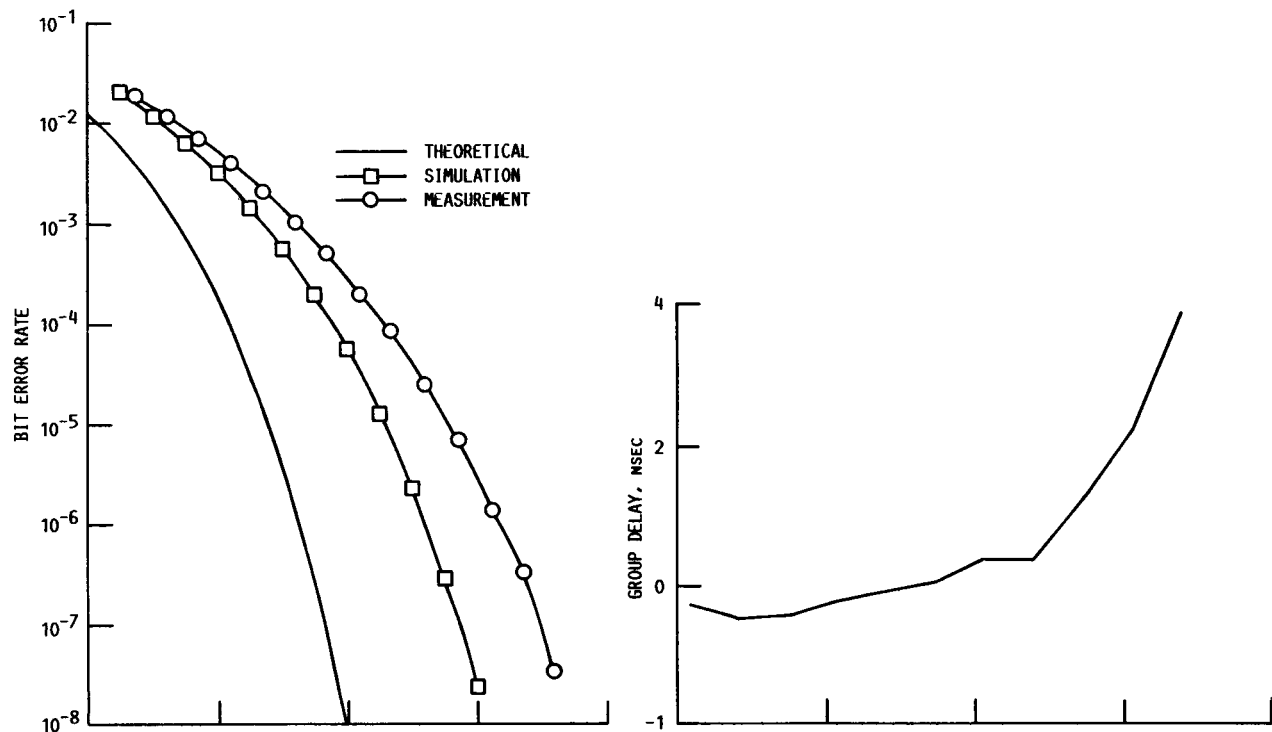
(F) BAND 3 - HIGH MODE - Xpt 3-3.

FIGURE 24. - CONTINUED.

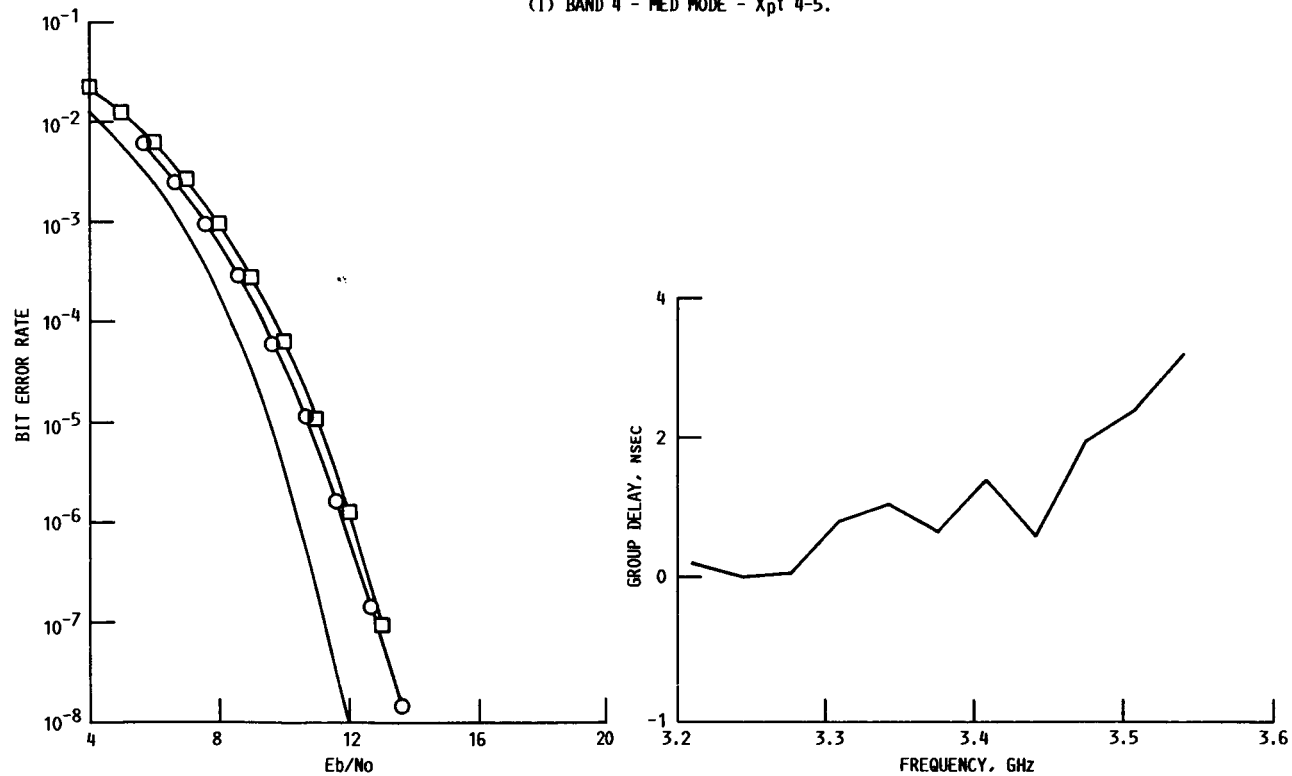(G) BAND 4 - LOW MODE - X_{pt} 6-7.

(H) BAND 4 - MED MODE - X_{pt} 3-3.

FIGURE 24. - CONTINUED.

(I) BAND 4 - MED MODE - Xpt 4-5.

(J) BAND 4 - HIGH MODE - Xpt 5-6.

FIGURE 24. - CONCLUDED.

37

1. Report No. NASA TM–89835	2. Government Accession No.	3. Recipient's Catalog No.		
4. Title and Subtitle A Study of the Effect of Group Delay Distortion on an SMSK Satellite Communications Channel		5. Report Date April 1987		
		6. Performing Organization Code 650-60-23		
7. Author(s) Robert J. Kerczewski		8. Performing Organization Report No. E-3491		
		10. Work Unit No.		
9. Performing Organization Name and Address National Aeronautics and Space Administration Lewis Research Center Cleveland, Ohio 44135		11. Contract or Grant No.		
		13. Type of Report and Period Covered Technical Memorandum		
12. Sponsoring Agency Name and Address National Aeronautics and Space Administration Washington, D.C. 20546				
		14. Sponsoring Agency Code		

15. Supplementary Notes

16. Abstract

The effects of group delay distortion on an SMSK satellite communications chan-nel have been investigated. Software and hardware simulations have been used to determine the effects of channel group delay variations with frequency on the bit error rate for a 220 Mbps SMSK channel. These simulations indicate that group delay distortions can significantly degrade the bit error rate performance. The severity of the degradation is dependent on the amount, type, and spectral loca-tion of the group delay distortion.

17. Key Words (Suggested by Author(s)) SMSK; Group delay; Satellite communications	18. Distribution Statement Unclassified – unlimited STAR Category 32		
19. Security Classif. (of this report) Unclassified	20. Security Classif. (of this page) Unclassified	21. No. of pages 38	22. Price* A03